EXPERIMENTAL FINDINGS AND NUMERICAL SIMULATIONS

ON

GASOLINE FUEL INJECTOR SYSTEM

by

Steven J. Wright

and

E. Benjamin Wylie

FINAL PROJECT REPORT

to

Bendix Research Labs
Southfield, Michigan

Jan. 17, 1980

Department of Civil Engineering
The University of Michigan
Ann Arbor, MI 48109

EXPERIMENTAL FINDINGS AND NUMERICAL SIMULATIONS

ON

GASOLINE FUEL INJECTOR SYSTEM

by

Steven J. Wright

and

E. Benjamin Wylie

FINAL PROJECT REPORT

to

Bendix Research Labs
Southfield, Michigan

Jan. 17, 1980

Department of Civil Engineering
The University of Michigan
Ann Arbor, MI 48109

TABLE OF CONTENTS

LIST OF FIGURES

LIST OF FIGURES CONTINUED

1. INTRODUCTION

This report provides documentation of the experimental and numerical investigations performed at The University of Michigan using the Bendix gasoline fuel injection system. The investigations were intended to examine the propagation of pressure waves in the fuel delivery system which are generated as a result of the fuel injector operation. Objectives of the study included a verification of the matched impedance approach to the reduction of pressure wave reflections in the system. Experimental and numerical simulations were conducted to demonstrate the approach. Another objective of the study was to examine the influence of the unsteady nature of the flow on the frictional resistance. Experiments in both laminar and turbulent flow were performed to consider the unsteady effects for the range of conditions expected in actual injector operation. Comparisons of the experimental data collected are made with computed numerical simulations and the results are critically examined.

This report describes the test apparatus used and its operating characteristics. Also presented are the equations used for the development of the numerical model. Included are the computer programs developed, and results of the program outputs are presented for comparison with the experimental data obtained.

2.0 EXPERIMENTAL APPARATUS

Description of System

The experiments were performed on the system supplied by Bendix. A complete description of all system components is not given herein. The apparatus basically consisted of a single fuel injector mounted on a length of stainless steel tubing with orifices and accumulators at the upstream and downstream ends. Fig. 2.1 is a schematic diagram of the system, with pertinent dimensions as listed. Several orifices were supplied by Bendix so that different flow conditions could be produced. Pressure signals were monitored by means of the two pressure transducers; one mounted directly above the fuel injector and the other was located approximately 6 inches upstream from the downstream orifice. The outputs from the transducers were connected to a dual beam storage oscilloscope and the corresponding outputs were recorded by taking a Polaroid photograph of the oscilloscope screen display. A typical record is given in Fig. 2.2 and consists of a trace of the electronic signal to operate the fuel injector solenoid (upper trace) and pressure traces from the two transducers (The middle trace is from the injector transducer and lower one is from the downstream transducer). The experiments were performed primarily with Stoddard solvent (specific gravity = 0.77 and kinematic viscosity = 1.17 centistokes at 25°C) as the working fluid.

A number of preliminary tests were conducted to establish the operating characteristics of the various system components. These were to provide the required inputs into the numerical

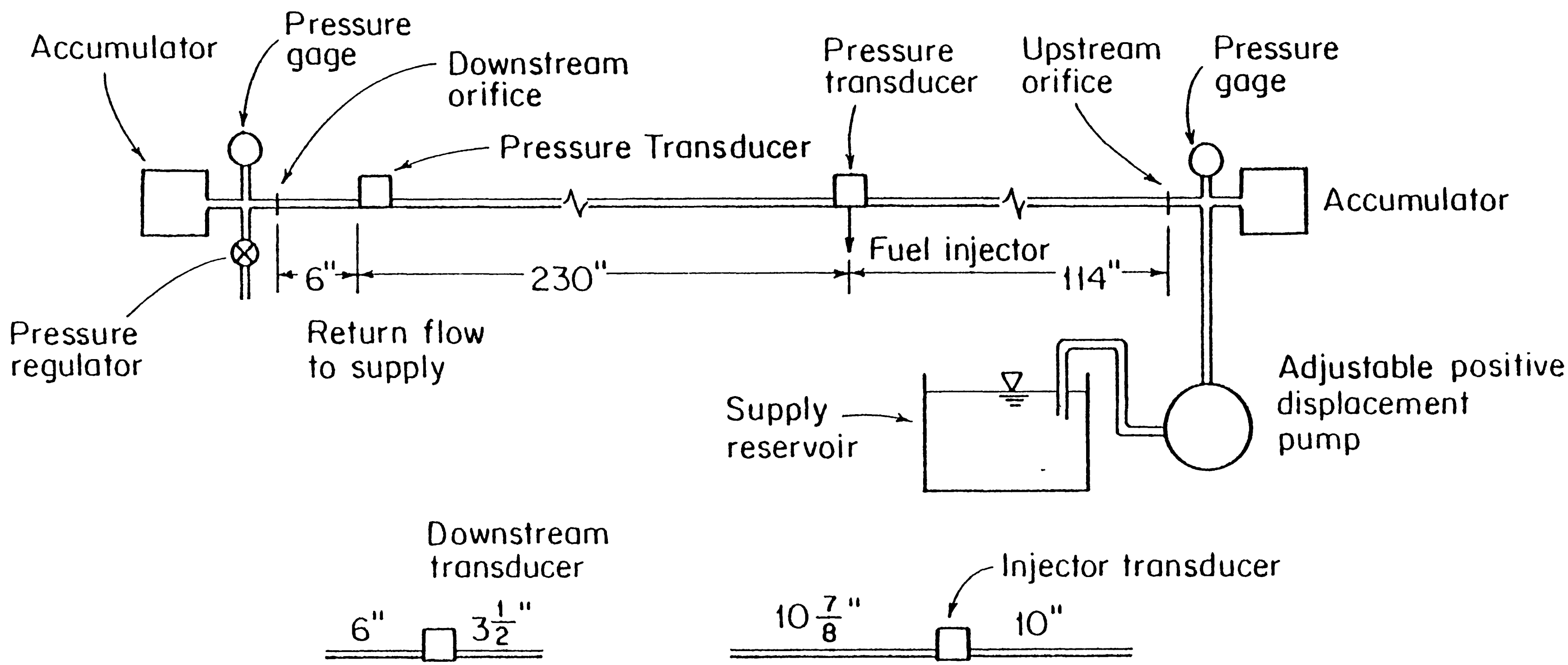

Lines shown are 0.305 in I.D.
all other lines in system are 0.312 in I.D.

Fig. 2.1. Schematic of experimental apparatus

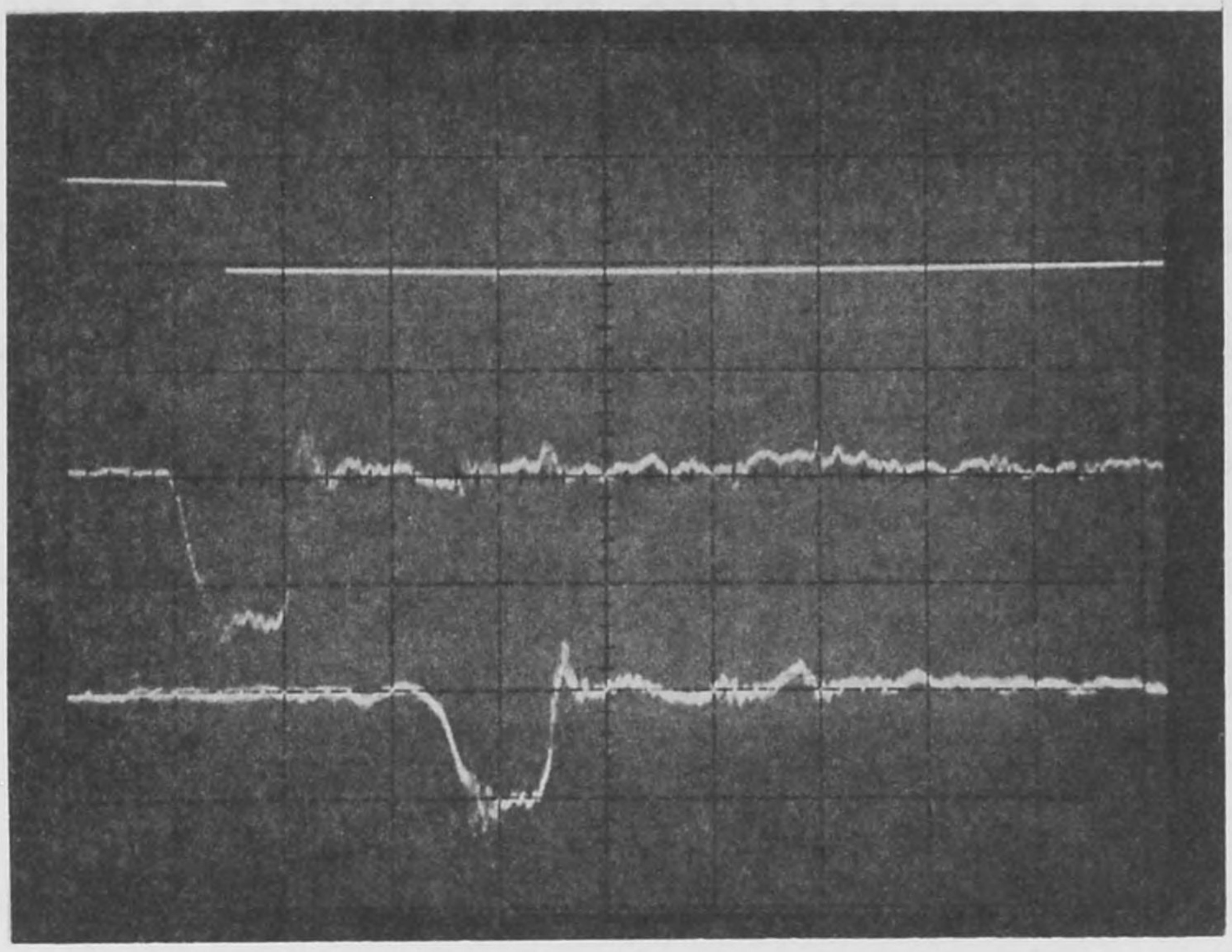

Fig. 2.2. Typical oscilloscope output.

simulations and to provide a basis for the interpretation of the experimental results.

The pressure transducers were calibrated so that pressure changes could be determined from the Polaroid photographs. The calibration procedure consisted of connecting the transducer to a dead weight tester, setting the oscilloscope to a fairly slow sweep period, lowering the known weight onto the test apparatus and storing the oscilloscope trace. This was repeated at several different pressure levels and the calibration factor was computed as the average of several tests. This procedure gave a calibration factor of 1.22 psi per millivolt of oscilloscope deflection for the transducer located at the injector and a factor of 1.05 psi/mv for the downstream transducer for the ranges of pressures examined during the actual experiments.

The discharge coefficients for the various orifices used in the experiments were measured for use in the numerical simulations. Since it was not possible to measure the orifice diameter accurately, the product $C_D A_o$ in the expression

$$Q = C_D A_o \sqrt{2g\frac{\Delta p}{\gamma}}$$

was determined since only the product was required for the numerical simulation. Here Q is the discharge, γ is the specific weight of the fluid, and Δp is the pressure difference across the orifice. This quantity was determined by disconnecting the tubing from the system at the upstream end and installing the orifice to be tested at that point. The pump pressure was adjusted to various levels and the orifice was discharged to atmospheric pressure. For each condition, the pressure level just upstream from the orifice was noted from the pressure gage and the discharge was determined by weighing a sample of fluid discharged in a given time period. All discharge coefficients ($C_D A_o$) were determined by an average of several tests and these were used in the numerical simulations.

Injector Characteristics

Other preliminary tests of interest were directed at determining the characteristics of the injector operation. The discharge coefficient (as given above) for the injector was determined in a similar manner. The orifice at the upstream end of the system was removed and replaced by a standard fitting so that relatively little energy loss would occur in the system. The downstream end was blocked off so that no flow would occur except through the injector which was operated in a continuously open condition. Again, by noting the upstream pressure, weighing a volume of fluid passed through the injector, and neglecting other losses, the discharge coefficient could be computed directly. The results of four tests at different pressure levels gave a discharge coefficient $C_D A_o$ of 2.6×10^{-6} ft^2 with a very small variation (less than 5 percent) between the different tests. This quantity was also used in the numerical simulations.

Another requirement for the simulation was the opening and closing characteristics of the injector. These were determined by running tests at different pressure levels across the system and obtaining test results for the pressure output from the transducer located at the injector. Results are presented in Fig. 2.3 a-c for pressure differences across the system of 8, 28, and 68 psi respectively. The different tests show no detectable variation in injector operation with pressure level so it was assumed that the opening and closing characteristics were independent of pressure level. The interpretation of the exact characteristics were hindered by the oscillations (discussed below) in the pressure trace, but the following conditions were observed; the opening was in a linear fashion (discharge increasing linearly) over a period of approximately 0.8 msec; the closure was also essentially linear except at the beginning of the closure when it appeared to close more slowly. For the purposes of the simulation, it was judged to be adequate to represent the closure as a linearly decreasing discharge over a time period of 0.3 msec. The description for the numerical simulations presented later was thus taken for any pulse width as an initial opening period of 0.8 msec where the injector opening increased linearly, a fully open period, and a 0.3 msec closure period with injector opening decreasing linearly to fully closed.

Even though the opening and closing characteristics of the injector appeared to be independent of pressure level, other operating parameters did appear to be strongly influenced by it. For example, the pressure oscillations mentioned above and visible in all of the figures occurred at different points of the injector operation sequence with different rail pressures. A sequence of experiments over a wide range of pressures is presented in

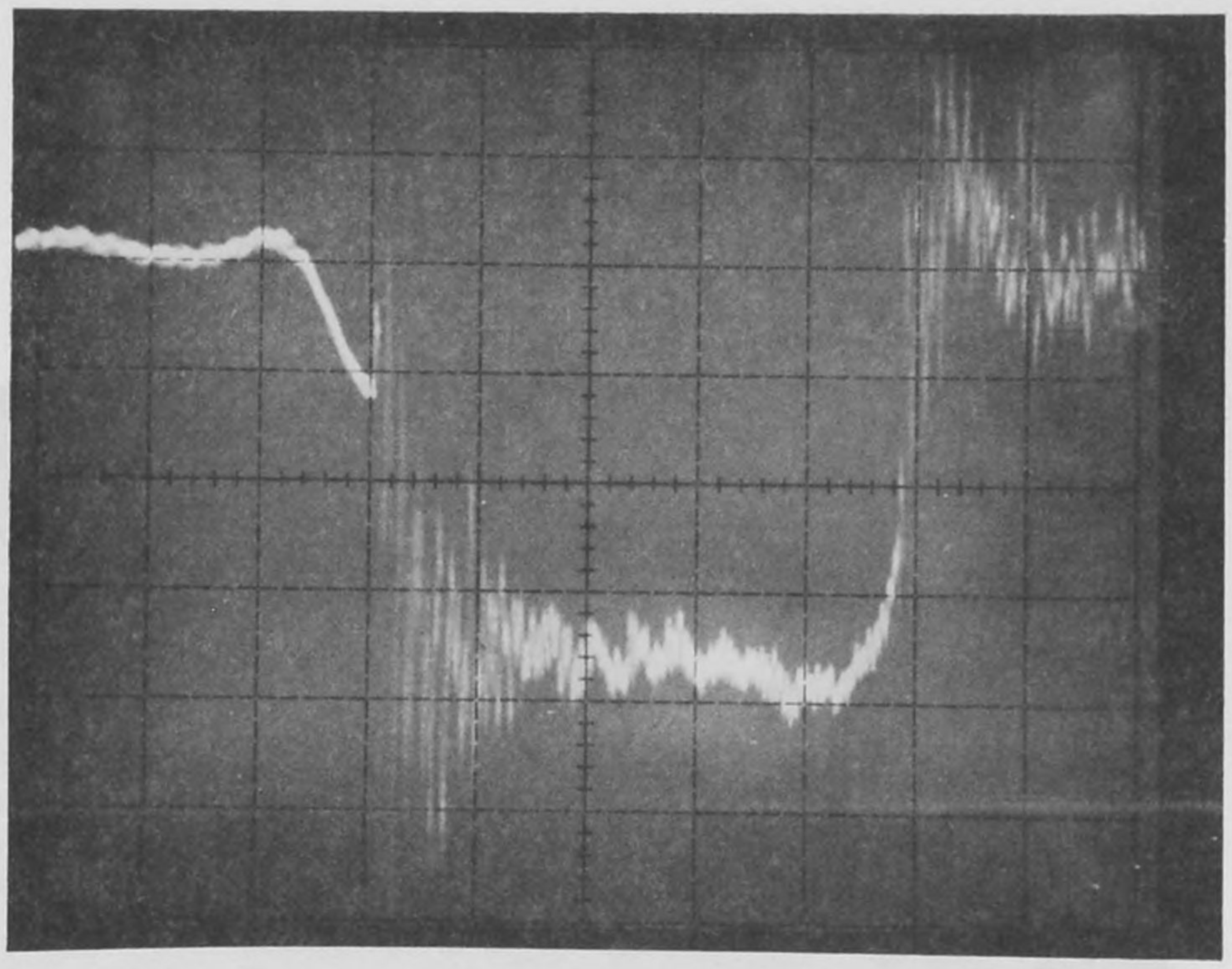

a) Upstream pressure - 40 psi. Downstream pressure - 32 psi.

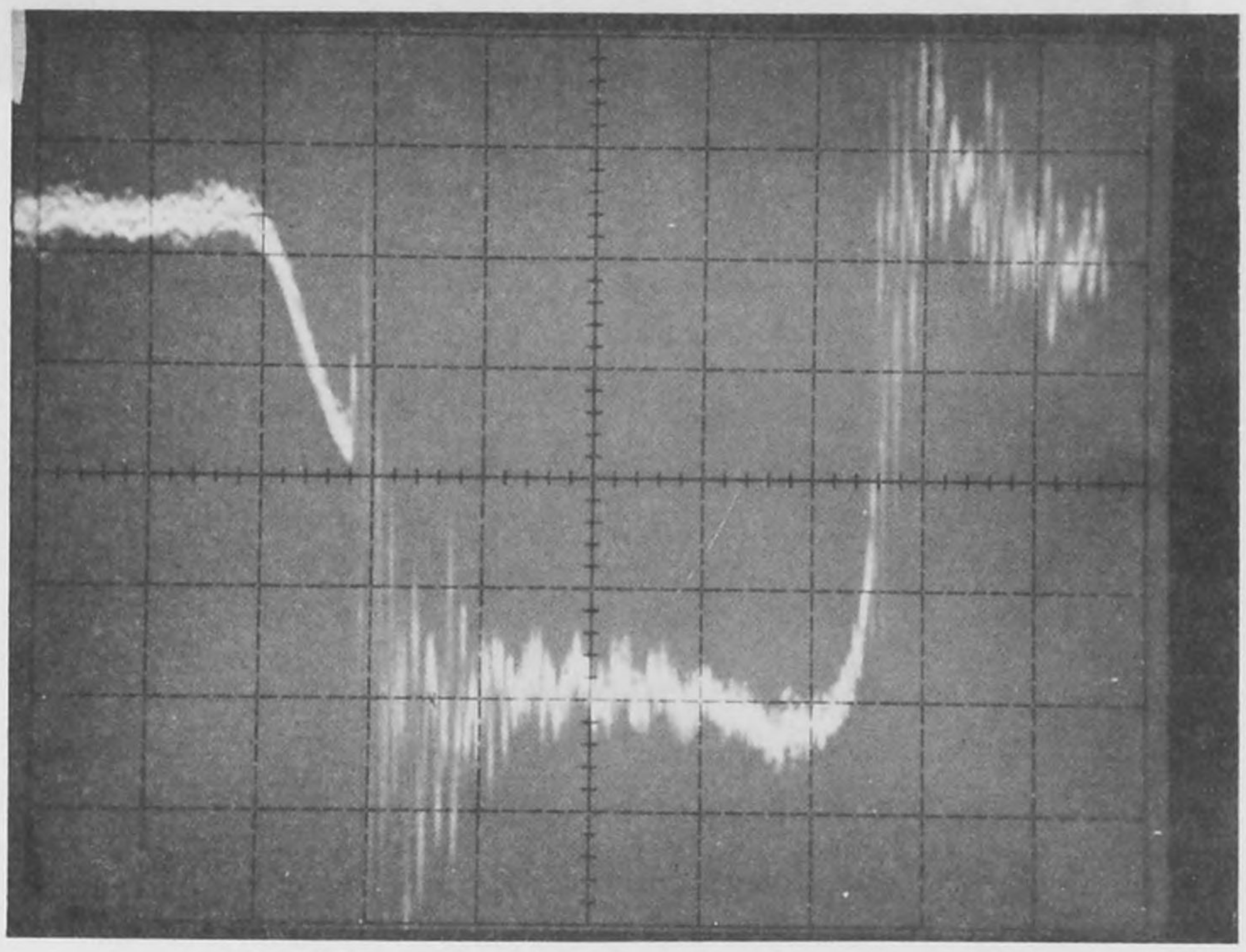

b) Upstream pressure - 60 psi. Downstream pressure - 32 psi.

Fig 2.3. Experiments to observe opening and closing characteristics of fuel injector (.5 ms/div. horizontal, 2 mv/div. vertical)

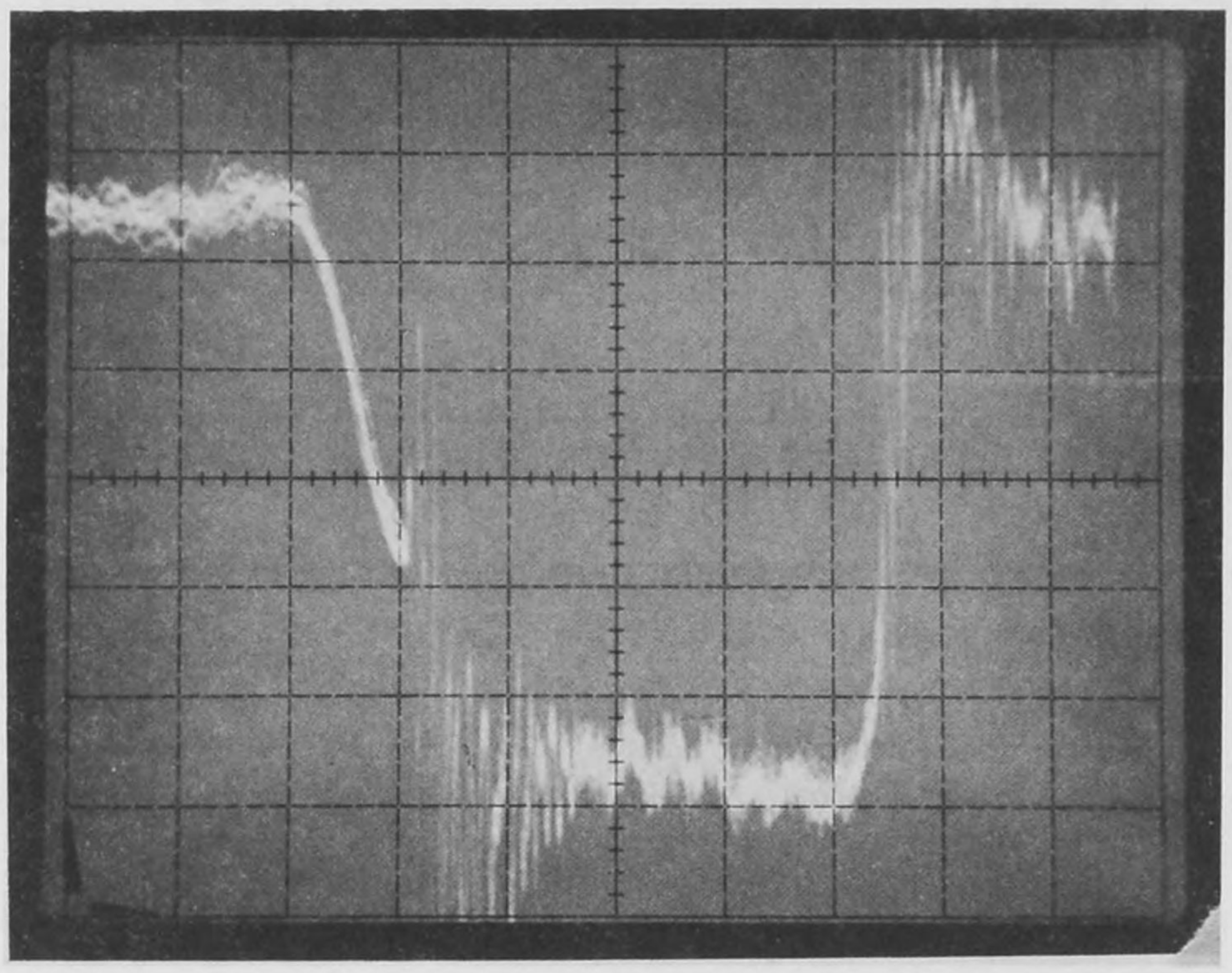

c) Upstream pressure – 100 psi. Downstream pressure 32 psi.

Fig. 2.3. (continued)

Fig. 2.4 with the conditions given. Various time intervals for the injector operation are indicated schematically in Fig. 2.5. The results for the experiments in Fig. 2.4 and additional experiments are presented in Table 2.1 and Fig. 2.6. Of particular interest to this study is the time interval Δt_4. This time interval decreases fairly rapidly with increasing pressure which results in a shorter open time for a particular pulse width. The reason for the injector behavior noted here is not understood since all of the mechanical characteristics have not been explored thoroughly.

An attempt was made to delineate the source of the oscillations shown in the figures above. These oscillations appeared on both the opening and closing sequences of the injector operation and propagated through the system since they can also be seen at the downstream transducer. In fact the occurrence of these oscillations as they reflect through the system provided an accurate means of identifying reflections from either end of the system. It was possible to remove the opening oscillation from the pressure signal if the electronic pulse width was shorter than a time interval approximately equal to 0.3 ms less than the time interval Δt_2. An example of this situation is given in Fig. 2.7. For longer pulse widths, the oscillations on the injector opening were unchanged. One thing noted was that when this oscillation was removed by shortening of the pulse width an audible click from the injector also vanished. Again, a total explanation of the operation is not understood although it is speculated that the oscillations are due to some

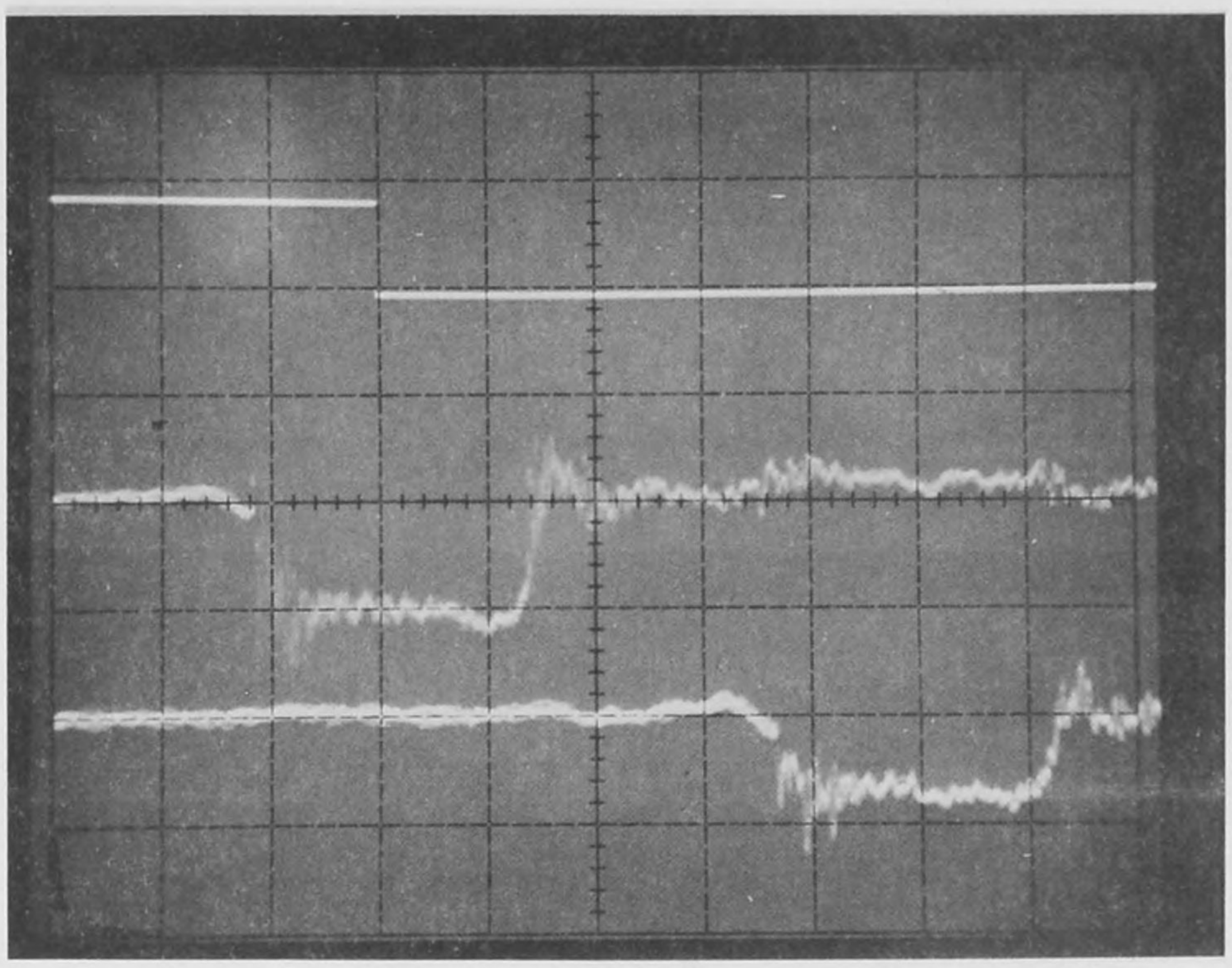

a) Injector pressure 21.5 psi

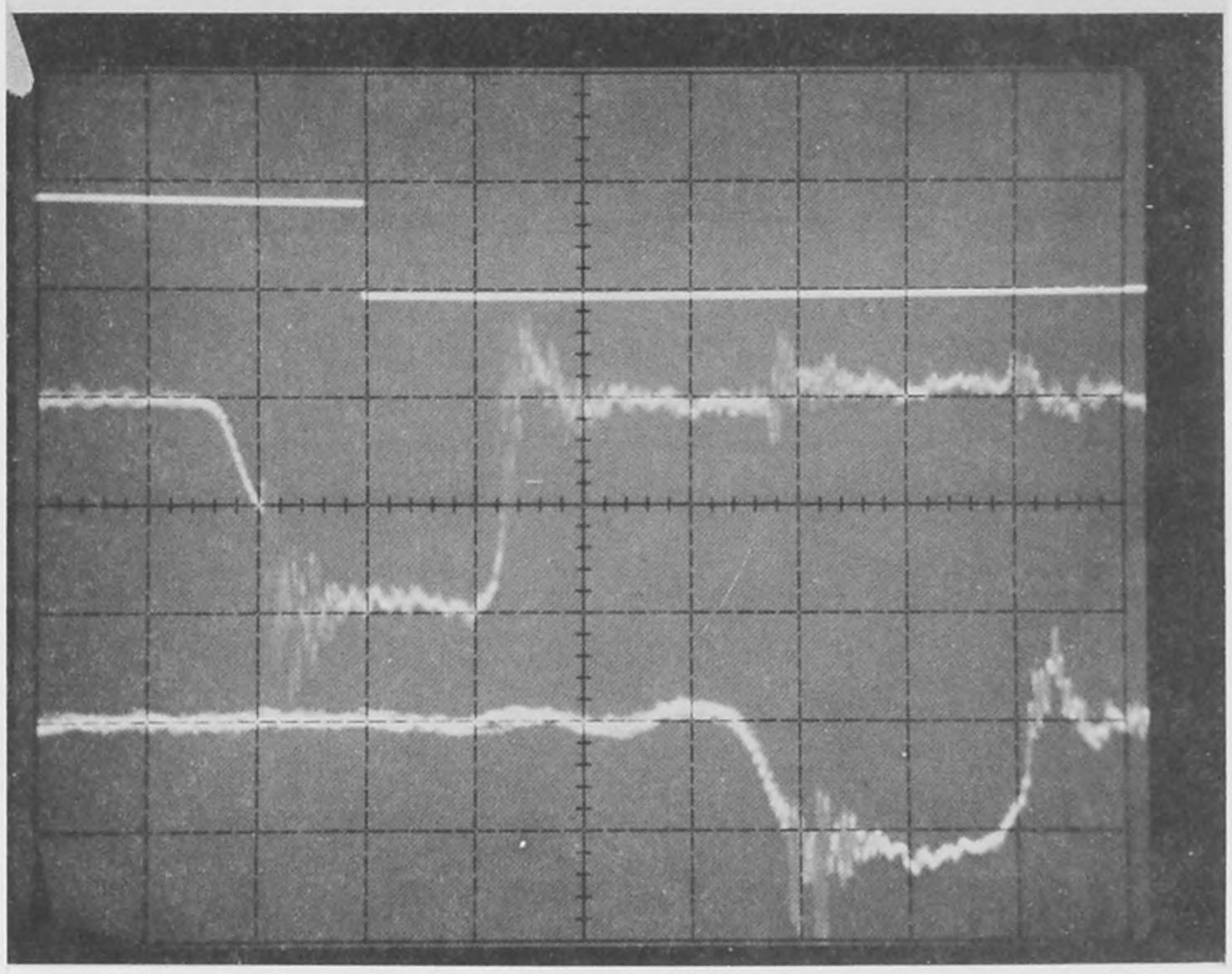

b) Injector pressure 51.5 psi

Fig. 2.4. Polaroid photocopy of injector operation characteristics as a function of pressure difference across fuel injection (1 ms/div. horizontal)

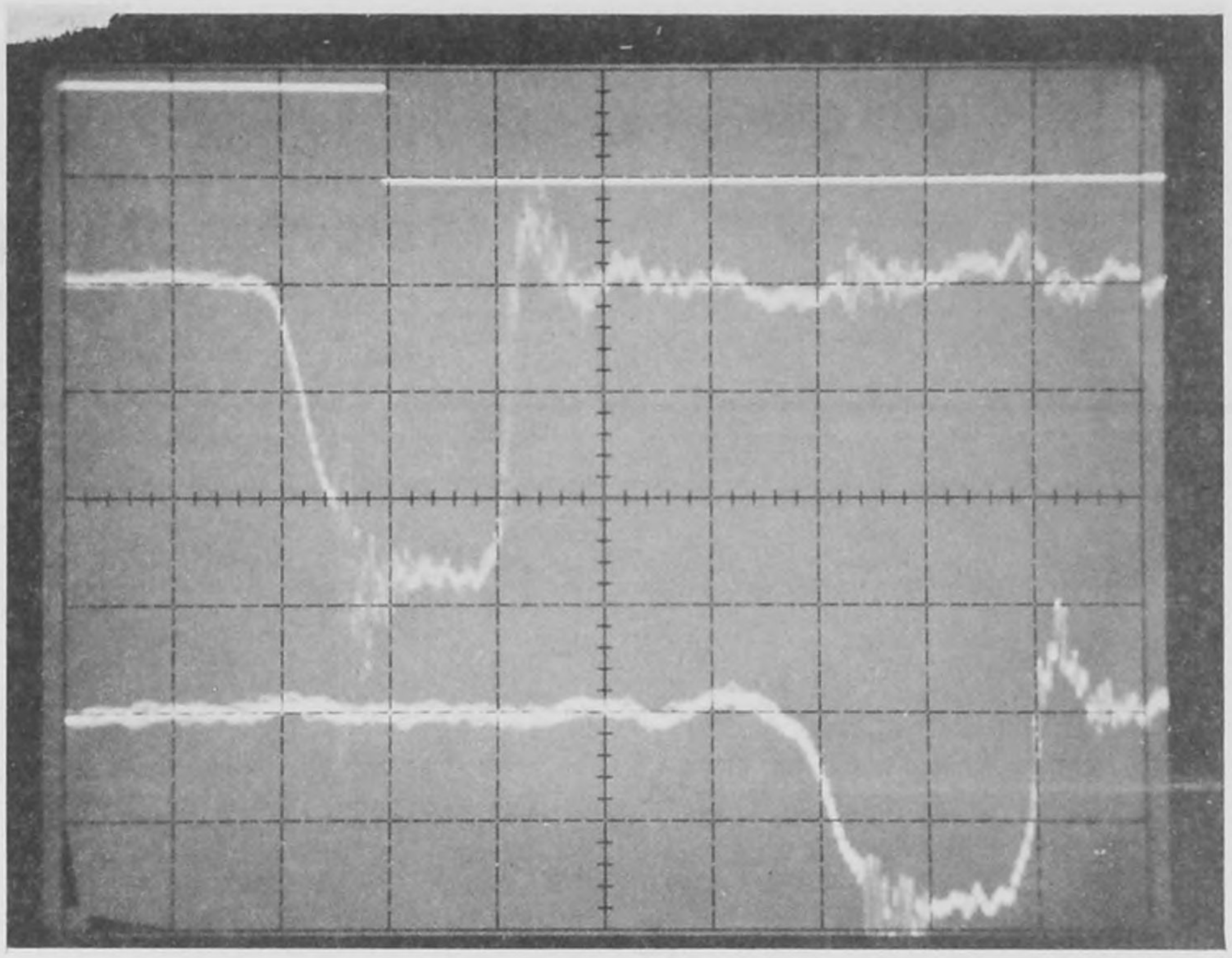

c) Injector pressure 105.8 psi.

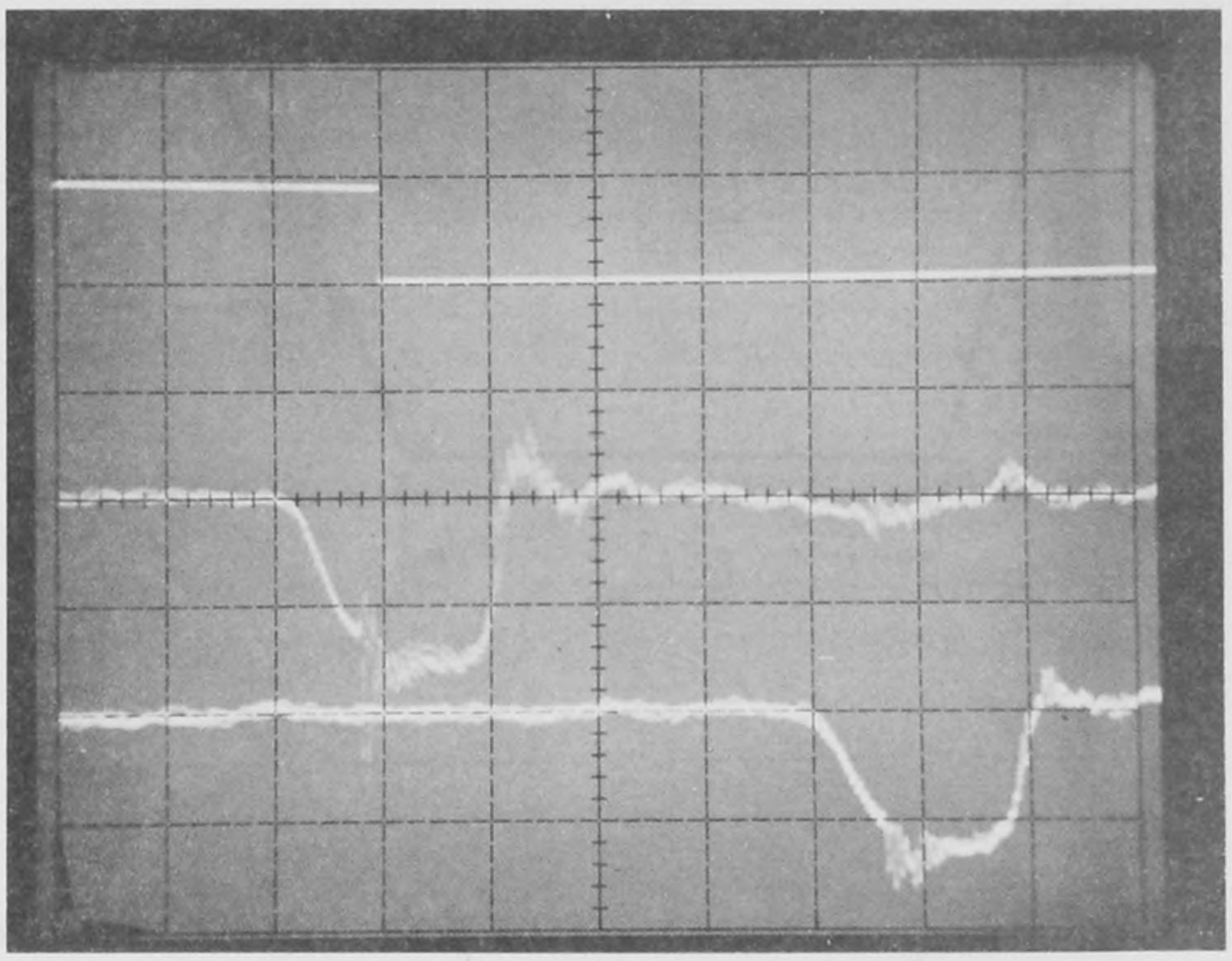

d) Injector pressure 128.8 psi.

Fig. 2.4. (continued)

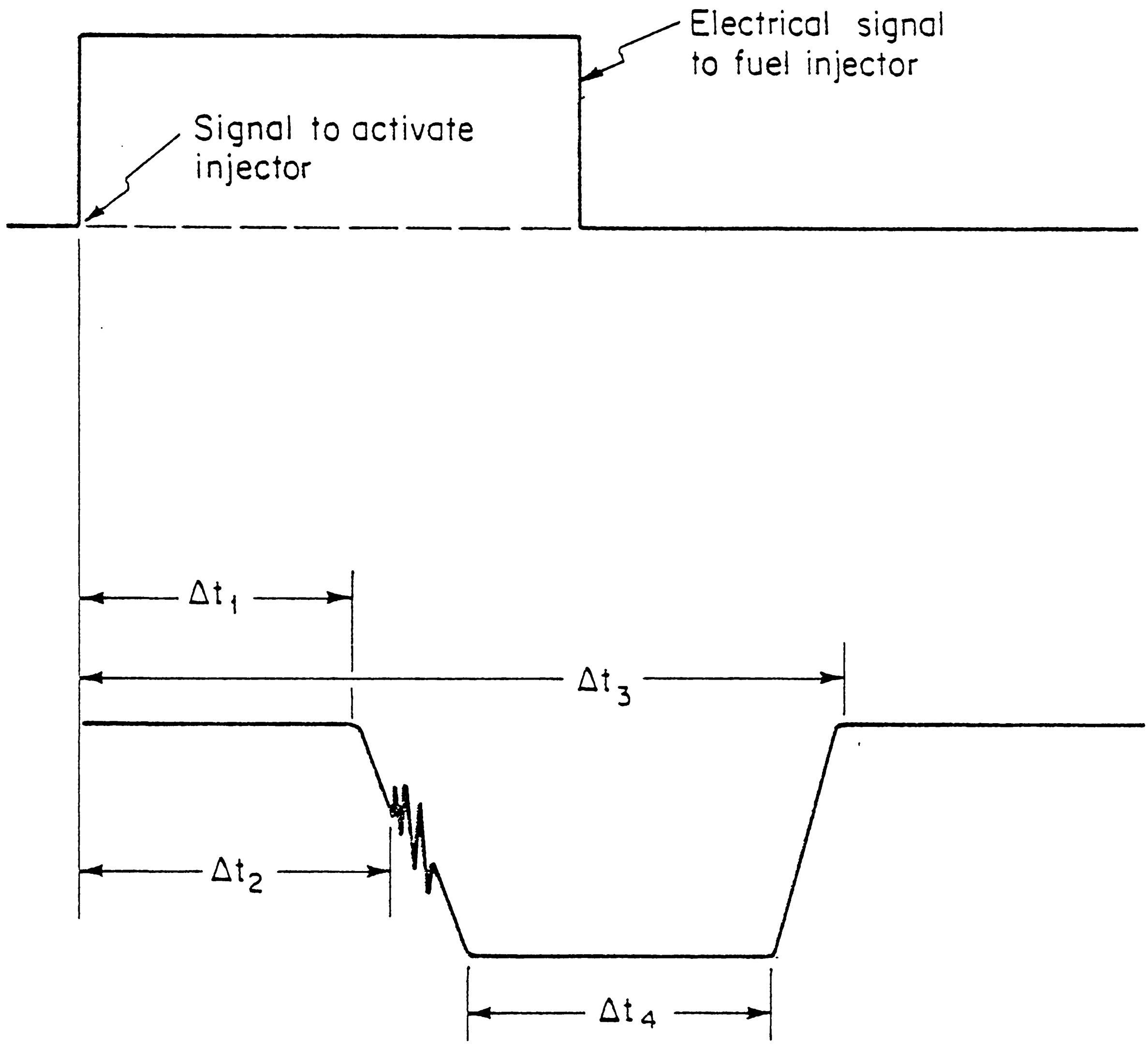

Fig. 2.5 Definition sketch for time intervals given in Table 2.1 and Fig. 2.6.

Table 2.1 Operating Characteristics of Fuel Injector as Function of System Pressures (pulse width 3 msec).

Upstream Pressure (psi)	Downstream Pressure (psi)	Injector Pressure (psi)	Δt_1 (msec)	Δt_2 (msec)	Δt_3 (msec)	Δ_4 (msec)
30	10	21.5	1.5	1.8	4.6	2.1
60	40	51.5	1.6	2.0	4.4	1.7
110	80	105.8	1.8	2.4	4.2	1.2
150	100	128.8	2.1	2.8	4.1	0.9
110	110	110	1.9	2.5	4.2	-
110	60	88.8	1.9	2.3	4.2	-
110	40	80.4	1.85	2.3	4.2	-
110	20	71.9	1.8	2.2	4.3	-
110	7	66.4	1.8	2.2	4.3	-

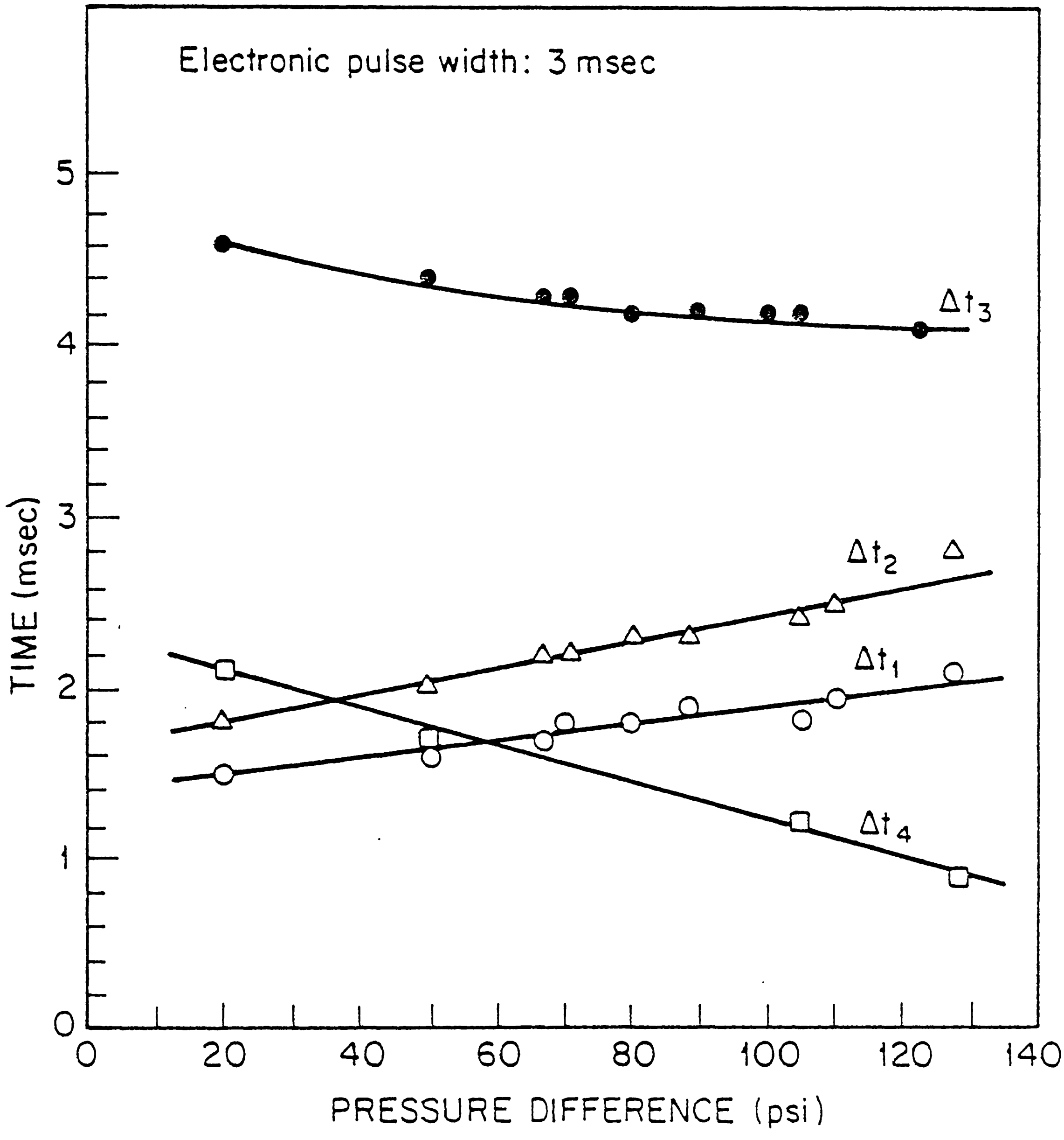

Fig. 2.6. Injector operation characteristics as a function of pressure difference across fuel injector.

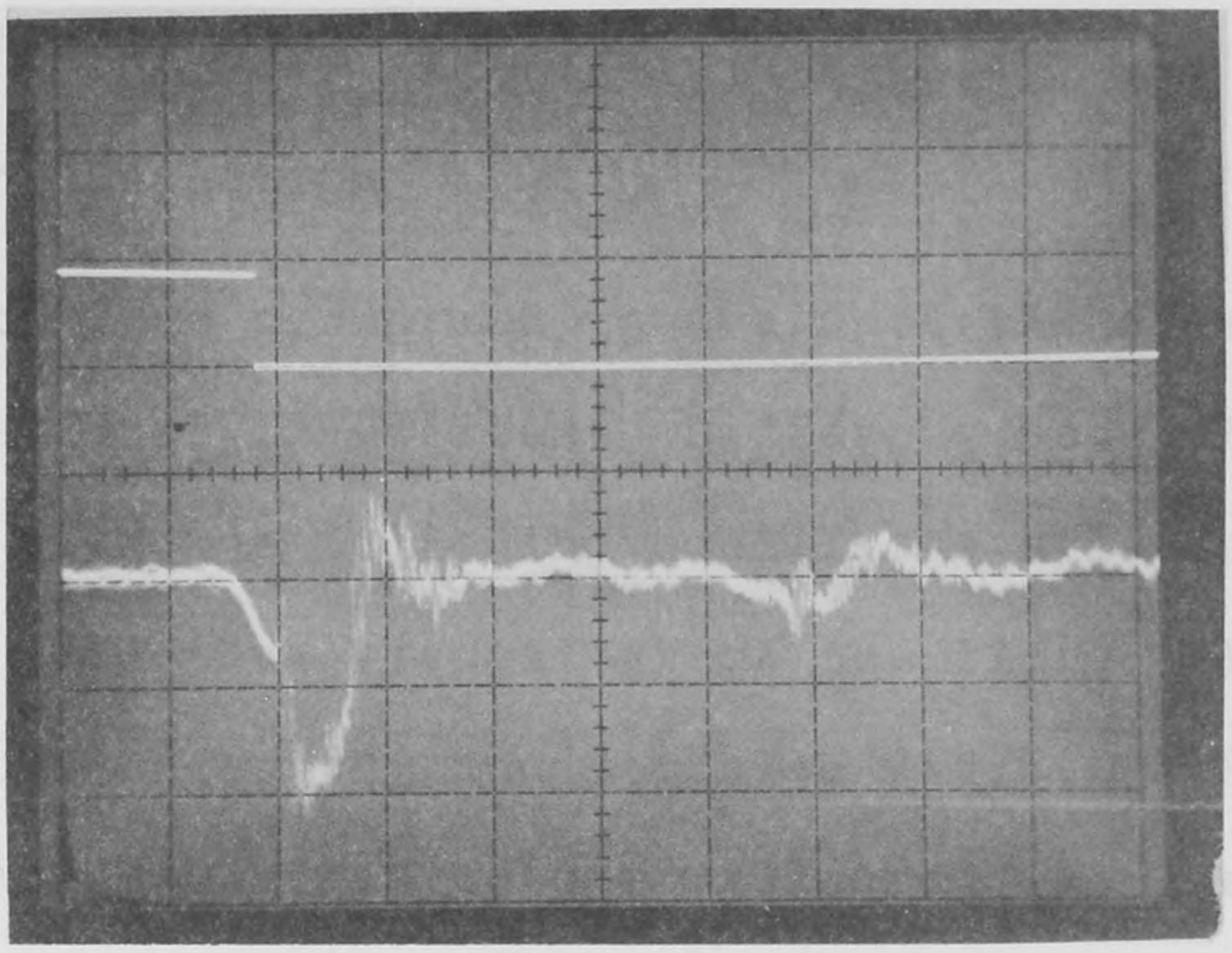

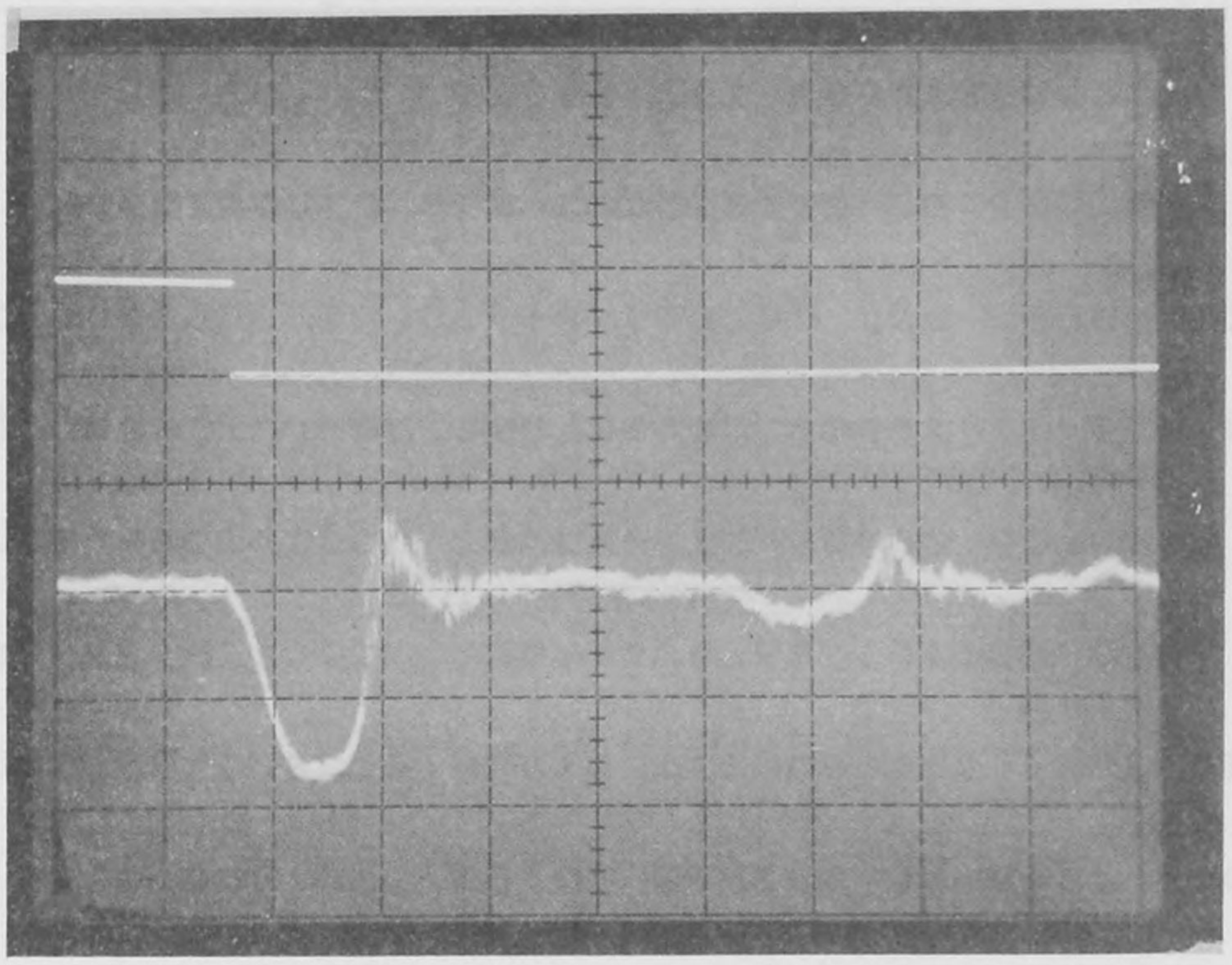

Fig. 2.7. Removal of initial oscillation by decreasing pulse width.

mechanical vibrations in the injector needle. These oscillations were observed to persist even if the injector was blocked at the outlet to prevent through-flow.

Repeatability of Injection

Experiments were performed to evaluate the general repeatability of individual injections. Different sets of experiments were performed with the following conditions held constant: 1) temperature (and thus viscosity) of the fluid; 2) pressure difference across injector; and 3) pulse width. A Mettler analytical balance accurate to one milligram was used to measure the injections. The fluid from a set of injections was caught in a flask and weighed.

This procedure was performed several times for various conditions (e.g. 20, 10, 5 pulses per measurement). The results of two sets of experiments are tabulated in Table 2.2. It is expected that the standard deviation of the measurements should increase with decreasing pulses/measurement if the results observed are due to random variation in the injected volume. Since this was not observed in either case, the variation must be due to other influences. Probable explanations are inaccuracies in reading the balance and the major source of variation which appeared to be due to fluid accumulation on the injector nozzle. This latter condition resulted in drops of 2-4 mg periodically shed during the injector operation. The variation of all measurements was basically within this 4 mg range and represents the probable explanation of the approximately constant standard deviations. The only conclusion that is justified from the experiments with this influence is that the standard deviation of individual injections is probably much smaller than that indicated and less than the resolution of the analytical balance.

Table 2.2 Results of Repeatability Measurements.

	Set 1				Set 2		
# of pulses	20	10	5	1	25	10	5
# of samples	21	21	21	21	12	14	20
standard deviation (gm)	.0016	.0011	.0017	.0008	.0012	.0015	.0011

3.0 NUMERICAL SIMULATIONS

The mathematical modeling of physical experiments was accomplished using a numerical simulation based upon the method of characteristics.* Since the method is reasonably well documented in the literature, the entire theory will not be repeated here. The equations in finite difference form as utilized in the computer programs are discussed in this section.

Figure 3.1 shows a schematic diagram of the physical apparatus as modeled, with the steady state hydraulic grade line indicated. The x-t plane is also shown with typical characteristic lines forming a staggered grid in the plane. Equal distance intervals, Δx, and time steps, Δt, to satisfy the Courant condition, $dx/dt = a$, in which a is the wave propagation velocity, are shown. The notation in Fig. 3.1 agrees with the notation in the programs listed in the Appendix.

The pipeline is divided into N equal reaches, which must be an even number for the staggered grid. The fuel injector is located at section NJS, which must be odd. The downstream orifice is located at section NS, an odd number equal to N+1. The upstream orifice is located at section 1. In addition to the pipeline and fuel properties, input data include the upstream and downstream pressures (assumed to remain constant) outside the orifices, and the discharge coefficient multiplied by the area of opening for each orifice. These data enable the steady through flow in the system to be computed.

---

*Wylie, E.B. and Streeter, V.L., FLUID TRANSIENTS, McGraw Hill, New York, N.Y., 1978.

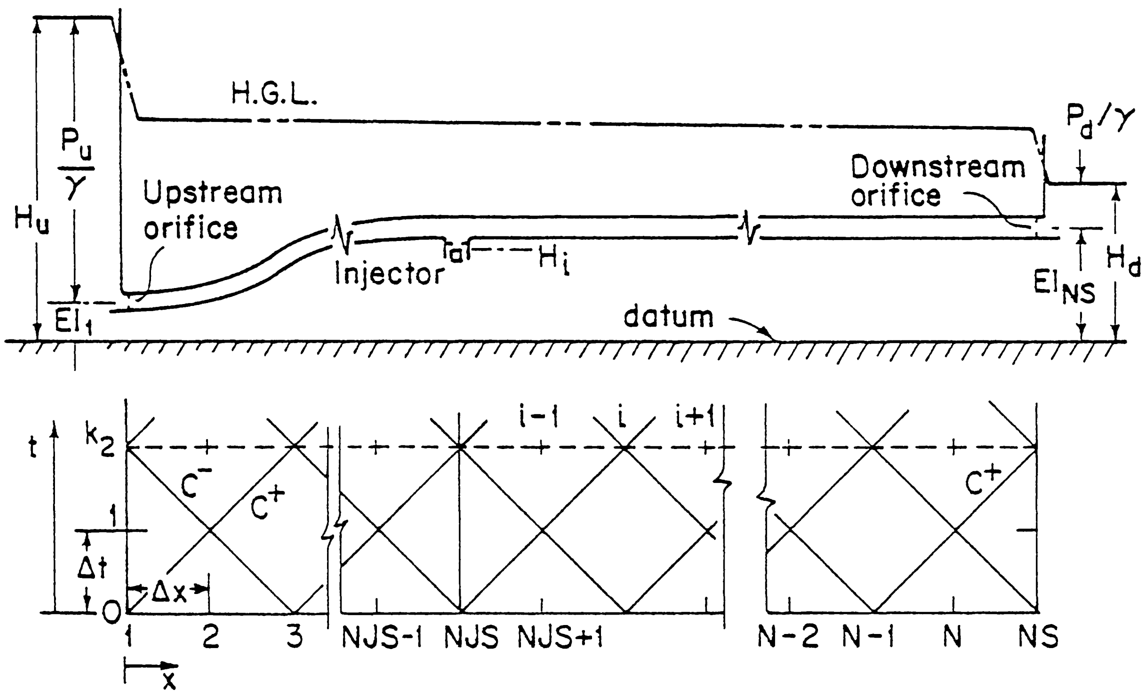

Fig. 3.1 Schematic diagram and xt plane

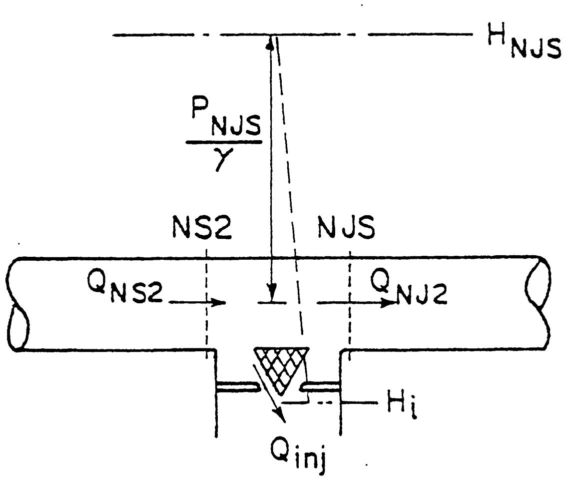

Fig. 3.2. Schematic diagram of injector flows and hydraulic gradeline.

Transient simulations are carried out by defining the repetitive period, PER = 60/rpm, of each injection cycle, and defining the dimensionless injector needle position vs time in tabular form. Thus the pulse width and the nature of the pulse can be defined (whether it is square or triangular in form). The discharge coefficient multiplied by open area of the injector is needed for the wide open position.

Method of Characteristics; Compatibility Equations

The two compatibility equations which relate the hydraulic gradeline elevation, H, and the discharge, Q, at adjacent sections, and which are valid along the C^+ and C^- characteristic lines are[1]:

$$H_i = C_P - B\ Q_i \tag{3.1}$$

$$H_i = C_M + B\ Q_i \tag{3.2}$$

in which $B = a/gA_r$, with A_r the pipe area, and

$$C_P = H_{i-1} + B\ Q_{i-1} - H_{fi-1} \tag{3.3}$$

$$C_M = H_{i+1} - B\ Q_{i+1} + H_{fi+1} \tag{3.4}$$

The subscribt i refers to the current time at section i while $i\pm1$ refers to one time-step earlier at the adjacent upstream (-) and downstream (+) sections. The last term in Eqs. (3.3) and (3.4) represents the viscous loss term. The energy dis-

[1]Wylie, E. B., and Streeter, V. L., FLUID TRANSIENTS, McGraw Hill, New York, N.Y., 1978.

sipation may be described in terms of a loss equivalent to steady-state flow at the same velocity, in which case, for turbulent flow,

$$H_{fi\pm1} = R\, Q_{i\pm1} \left|Q_{i\pm1}\right| \tag{3.5}$$

with $R = f\, \Delta x/(2gDA_r^{\,2})$. The Darcy Weisbach friction factor is given by f, and the fuel rail diameter by D. For laminar flow,

$$H_{fi\pm1} = 32\nu\ \Delta x\ Q_{i\pm1}/(gD^2A_r) \tag{3.6}$$

in which ν is the fluid kinematic viscosity. Alternatively, for laminar flow, the dependence of the viscous losses upon the unsteady nature of the velocity profile can by incorporated in the compatibility equations[1]. In this case

$$H_{fi\pm1} = \bar{H}_{fi\pm1} + H'_{fi\pm1} \tag{3.7}$$

in which $\bar{H}_f$ is given by Eq. (3.6), the steady-state friction loss equation, and H'_f is the deviation from the steady-state value due to the unsteady motion of the fluid. Although this latter refinement is incorporated in the program for laminar flow, Appendix A, little modification in computational results occur as a result of the refinement. This is because of the dominance of the orifice losses on the response in this operating system. Additional discussion of frequency dependent friction is included at the end of this section, prior to the introduction of the computer program.

At all interior computational sections in the fuel rail the instantaneous hydraulic gradeline and flow rate are given

---

[1] Zielke, W, "Frequency-Dependent Friction in Transient Pipe Flow," J. Basic Engr., Trans. ASME, Vol. 90, Ser D, No. 1 pp. 109-115, March, 1968.

by a simultaneous solution of Eqs. (3.1) and (3.2)

$$H_i = (C_P + C_M)/2 \tag{3.8}$$

$$Q_i = (H_i - C_M)/B \tag{3.9}$$

Boundaries. Upstream Orifice.

Positive flow through the upstream orifice is described by

$$Q_1 = C_D A_u \sqrt{2g(H_u - H_1)} \tag{3.10a}$$

and negative flow, by

$$Q_1 = -C_D A_u \sqrt{2g(H_1 - H_u)} \tag{3.10b}$$

The fuel rail response during transient flow is conveyed to the orifice along the C^- characteristic line and is described by Eq. (3.2). For positive flow simultaneous solution of Eqs. (3.2) and (3.10a) yields

$$Q_1 = -C_V B + \sqrt{(C_V B)^2 + 2C_V(H_u - C_M)} \tag{3.11a}$$

and for negative flow, Eqs. (3.2) and (3.10b) yield

$$Q_1 = C_V B - \sqrt{(C_V B)^2 - 2C_V(H_u - C_M)} \tag{3.11b}$$

in which $C_V = g(C_D A_u)^2$. Examination of these equations shows that Eq. (3.11a) will yield positive flow only when $(H_u - C_M) > 0$, and Eq. (3.11b) will yield negative flow only when $(H_u - C_M) < 0$. Thus by setting S = 1 for the first case and S = -1 for the second case the following equation handles both conditions.

$$Q_1 = S(-C_v B + \sqrt{(C_v B)^2 + 2SC_v(H_u - C_M)}) \tag{3.12}$$

Once Q_1 is determined in Eq. (3.12), the hydraulic gradeline at section 1 is calculated using Eq. (3.2).

Downstream Orifice.

Positive flow through the downstream orifice is given by

$$Q_{NS} = C_D A_D \sqrt{2g(H_{NS} - H_D)} \tag{3.13a}$$

and negative flow by

$$Q_{NS} = -\ C_D A_D \sqrt{2g(H_D - H_{NS})} \tag{3.13b}$$

Simultaneous solution of each of these equations with the C^+ compatibility Eq. (3.1), with $S = 1$ for $(C_P - H_D) > 0$ and $S = -1$ for $(C_P - H_D) < 0$, yields

$$Q_{NS} = S\ (-C_{vD} B + \sqrt{(C_{vD} B)^2 + 2SC_{vD}(C_P - H_D)}\ ) \tag{3.14}$$

In Eq. (3.14) $C_{vD} = g(C_D A_D)^2$. Equation (3.1) is used to find the hydraulic grade line in the fuel rail at the downstream orifice, H_{NS}, after Q_{NS} is determined in Eq. (3.14).

Fuel Injector.

Flow through the fuel injector, Fig. 3.2, is given by

$$Q_{inj} = C_D A_i \sqrt{2g(H_{NJS} - H_I)} \tag{3.15}$$

Inasmuch as the injector needle may not open instantaneously, and therefore an intermediate needle position may be needed, a dimensionless ratio is used to define the needle position

$$\tau = \frac{C_D A_I}{(C_D A_I)_o} \qquad (3.16)$$

The subscript o refers to the product of the discharge coefficient and area of opening in the wide open position. The combination of Eqs. (3.15) and (3.16), with $C_I = (C_D A_I)_o \sqrt{2g}$, yields

$$Q_{inj} = \tau \, C_I \sqrt{H_{NJS} - H_I} \qquad (3.17)$$

A common pressure is assumed in the fuel rail at the injector, H_{NJS}, and at any instant continuity of flows at the injector may be stated, Fig. 3.2,

$$Q_{NS2} - Q_{inj} - Q_{NJS} = 0 \qquad (3.18)$$

When Eqs. (3.17), (3.18), Eq. (3.1) for the upstream side of the injector, and Eq. (3.2) for the downstream side of the injector, are combined, and solved for the hydraulic grade line:

$$H_{NJS} = (A_1 - \sqrt{A_1 - (C_P + C_M)^2 - B^2 C_I^2 \tau^2 H_L}) \;/2 \qquad (3.19)$$

In Eq. (3.19), $A_1 = C_P + C_M + (BC_i\tau)^2/4$. When the injector needle is closed, $\tau = 0$, and Eq. (3.19) reduces to Eq. (3.8). Once H_{NJS} has been determined the individual flows at the injector may be determined from Eqs. (3.17), (3.1), and (3.2).

Frequency-Dependent Friction

Inasmuch as energy loss due to fluid friction is highly dependent upon the rate of change of velocity, it follows that waves that contain higher harmonics attenuate much faster than low frequency components. For unsteady laminar flow Zielke[2] developed a procedure to correct the steady-state friction term in the method of characteristics. In Eq. (3.7), H_f', which represents the deviation from the steady-state value of friction loss, is evaluated based on the history of the velocity at the section. In integral form the correction is expressed

$$H_f' = \frac{16\nu}{gD^2A_r} \int_0^t \frac{dQ}{dt}(u)W(t-u)\,du \qquad (3.20)$$

in which W is a weighting function which is a function of time. For convenience it is expressed in terms of dimensionless time τ,

$$\tau = \frac{4\nu}{D^2} t \qquad (3.21)$$

and is calculated by the use of two different series of terms, one for values of $\tau > 0.02$, and the other for values of $\tau < 0.02$. The two series provide overlapping values in the vicinity of $\tau = 0.02$.

$$W(\tau) = e^{-26.3744\tau} + e^{-70.8493\tau} + e^{-135.0198\tau} + e^{-218.9216\tau} + e^{-322.5544\tau} \quad \tau > 0.02 \qquad (3.22a)$$

---

[2] Zielke, W. "Frequency-Dependent Friction in Transient Pipe Flow," J. Basic Engr., Trans. ASME, Vol. 90, Ser. D, No. 1, pp. 109-115, Mar., 1968.

$$W(\tau) = 0.282095\,\tau^{-\frac{1}{2}} - 1.25 + 1.057855\tau^{\frac{1}{2}} + 0.9375\tau + 0.396696\tau^{3/2}$$

$$- 0.351563\tau^2 \qquad \tau < 0.02 \qquad (3.22b)$$

In the application of the method of characteristics, Eq. (3.20) is evaluated from a first-order approximation by using the history of the velocity and the weighting function in the following manner.

$$H'_{fi,k} = \frac{16\nu}{gD^2A_r} \sum_{j=1}^{k_m} (Q_{i,j+1} - Q_{i,j})\ W((2(k_m + 1 - j)-1)\Delta t)$$

$$= \frac{16\nu}{gD^2A_r} \sum_{j=1}^{k_m} (Q_{i,k_m+2-j} - Q_{i,k_m+1-j})\ W((2j-1)\Delta t) \quad (3.23)$$

By referring to the grid in Fig. 3.3, Eq. (3.23) can be written

$$H'_{fi,k} = \frac{16\nu}{gD^2A_r} \quad (Q_{i,k_m+1} - Q_{i,k_m})\ W(\Delta t) + (Q_{i,k_m} - Q_{i,k_m})W(3\Delta t)$$

$$+ \ . \ . \ . + (Q_{i,2} - Q_{i,1})W((2k_m - 1)\Delta t \qquad (3.24)$$

The weights W are calculated from Eqs. (3.22a) and (3.22b) as functions of the dimensionless parameter τ. The numerical value of $W(\tau)$ approaches zero as τ becomes very large. If a value of τ_{max} is selected such that all weights $W(\tau)$ for $\tau > \tau_{max}$ are negligible, then the number of terms in Eq. (3.24) never exceeds $\tau_{max}D^2/(8\nu\Delta t)$.

As stated earlier, the introduction of the frequency-dependent losses in this particular problem made little difference in the

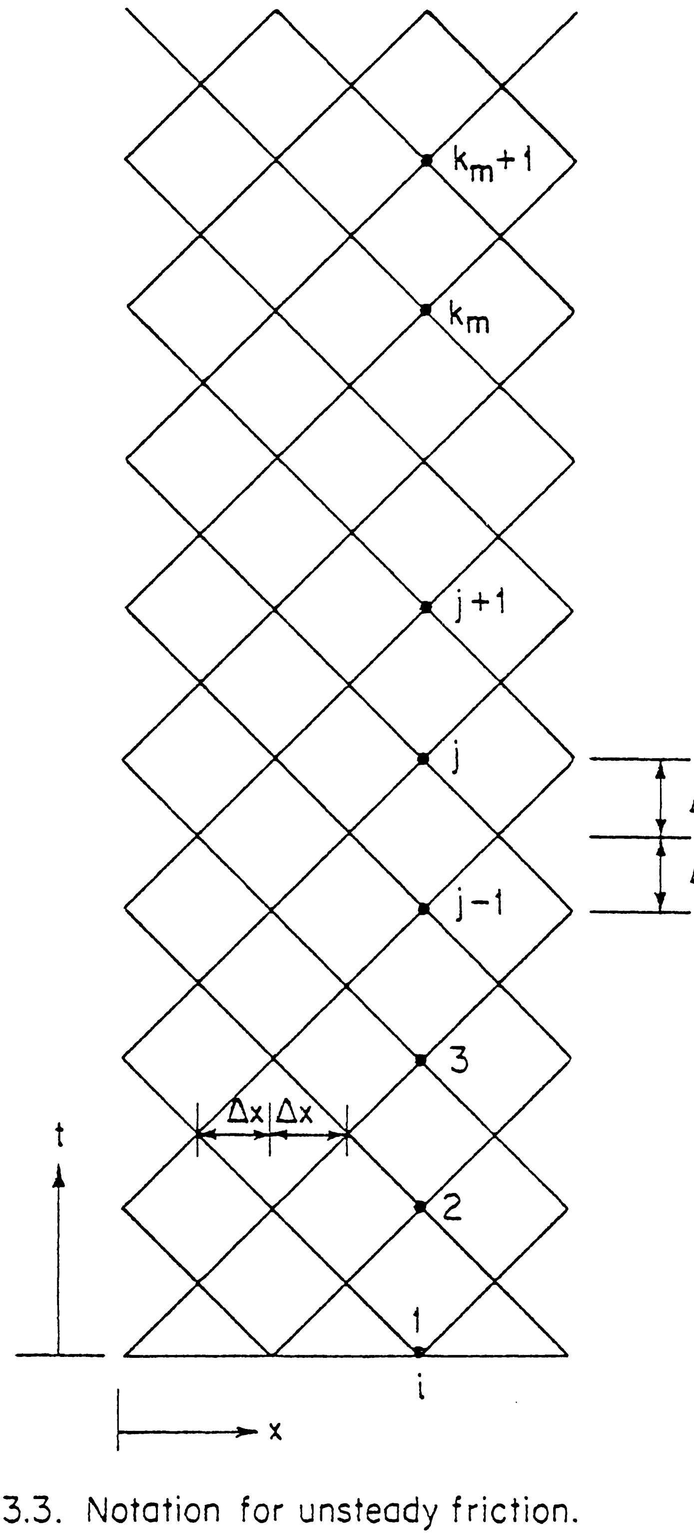

Fig. 3.3. Notation for unsteady friction.

calculated response for laminar flow. This is because the pipeline losses are much smaller than other system losses, namely the orifice losses, which totally dominate the system dissipation.

The relative importance of the frequency dependent friction effects for typical fuel injection systems can be estimated by considering the magnitude of the friction term to other terms in the characteristic equations. Specifically consider the ratio

$$\frac{gH_f A_r}{\frac{dQ}{dt}} \tag{3.25}$$

for the case of a linear drop (or rise) in pressure in time Δt (e.g. associated with opening and closing of injector). This results in change of flow ΔQ in the same time period. Take a typical value of Δt on the order of 1 msec, ν of 1.0×10^{-5} ft^2/sec; and D of 0.3". Then the major contribution to the unsteady friction term would be associated with the maximum change in discharge

$$H_f' \approx \frac{16\nu}{gD^2 A_r} \Delta Q \; W(\tau) \tag{3.26}$$

For $\tau = 4\nu\Delta t/D^2 = 6.4 \times 10^{-5}$ then $W(\tau) = 34.$ and the unsteady friction term is much larger in magnitude than the steady state friction term provided that ΔQ and Q are of the same order of magnitude or if ΔQ is greater than Q. The ratio in Eq. (3.25) is thus given approximately by

$$\frac{gH_f A_r}{\frac{dQ}{dt}} \approx W(\tau)\tau \tag{3.27}$$

The maximum value of this ratio is for τ on the order of .02 and is 0.072 For the value of τ above, the value is .0088 Thus it can be seen for the first reflection where only one or two terms in the unsteady friction are important, that the unsteady friction is small relative to other terms in the characteristic equations, and it should be expected that significant unsteady friction effects should not become apparent until there have been several reflections through the system. Although this conclusion is only valid for laminar flow, it is presumed that a similar conclusion would be justified for turbulent flow. Since there is no theoretical development for frequency dependent friction effects in turbulent flow, this hypothesis cannot be verified mathematically.

Two programs in FORTRAN are provided in the Appendix. The first is for laminar flow and includes the frequency dependent losses. The second is essentially the same program except it is for turbulent flow and includes viscous losses evaluated using the Darcy-Weisbach equation, with the friction factor evaluated as a function of the local mean velocity utilizing the Colebrook Equation. A sample output is provided along with a list of variables in the programs.

4.0 THE FUEL RAIL WITH MATCHED IMPEDANCES AT THE TERMINALS

The equations that describe the transient behavior of the fuel rail are identified below, and the variables and controlling parameters in the problem are discussed.

Transient Pipeline Equation: Since viscous losses along the pipeline are minor compared with losses at the terminal orifices, the flow delivered when the injector opens is derived equally from each side of the injector. If the injector flow is $2\Delta Q$ then $\Delta p = \pm \gamma B \Delta Q$ describes the transient behavior in the fuel rail during fuel injection. Δp is the pressure drop, $\gamma = \rho g$ is the unit weight of the fluid with ρ the mass density, $B = a/gA_r$ is the characteristic impedance of the pipeline in which a is the wave propagation velocity and A_r is the pipe cross-sectional area. In terms of the variables shown in Fig. 4.1 the wave propagation in the fuel rail is described by

$$H_o - H = B \Delta Q \tag{4.1}$$

Orifices: Flows through the orifices are described by the following relationships. In each case the coefficient $C = KA_o\sqrt{2g}$, in which K is the orifice discharge coefficient and A_o is the flow area.

Injector:

$$2 \Delta Q = C_I \sqrt{H - H_I} \tag{4.2}$$

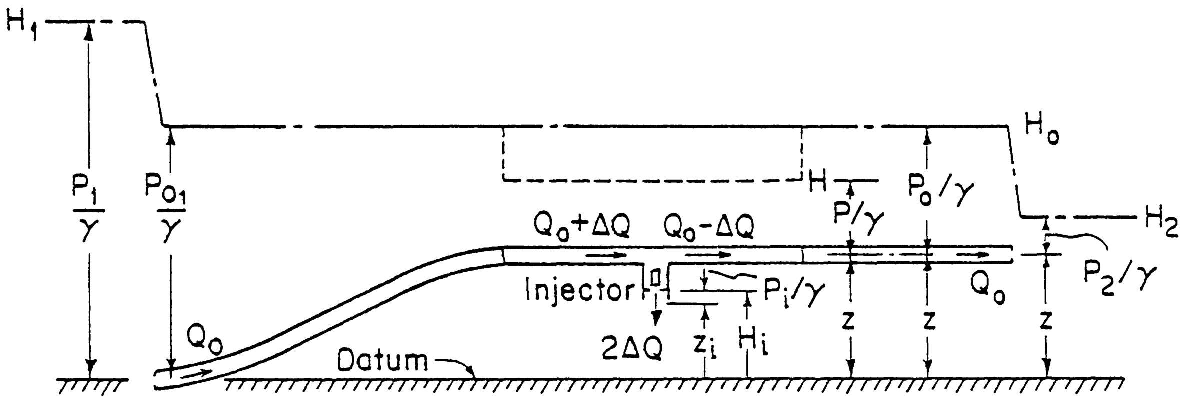

Fig. 4.1. Fuel Rail

Upstream orifice:

$$Q_o = C_u\sqrt{H_1 - H_o} \qquad (4.3)$$

$$Q_o + \Delta Q = C_u\sqrt{H_1 - H} \qquad (4.4)$$

Downstream orifice:

$$Q_o = C_d\sqrt{H_o - H_2} \qquad (4.5)$$

$$Q_o - \Delta Q = C_d\sqrt{H - H_2} \qquad (4.6)$$

Equations (4.4) and (4.6), with H defined in Fig. 4.1, are valid only for the condition of no reflection at the orifice.

Controlling Parameters and Variables: There are eleven variables and parameters that dictate the behavior of the fuel injector.

B : the pipeline impedance = a/gA_r

C_I: the injector coefficient = $K_i A_{oi}\sqrt{2g}$

C_u: the upstream orifice coefficient = $K_u A_{ou}\sqrt{2g}$

C_d: the downstream orifice coefficient = $K_d A_{od}\sqrt{2g}$

Q_o: the fuel rail flow rate

ΔQ: one-half of the injector flow rate

H_o or $(p_o/\gamma+Z)$: the hydraulic grade line elevation along the fuel rail

H_1 or $(p_1/\gamma+Z)$: the hydraulic grade line on the upstream side of the upstream orifice

H_2 or $(p_2/\gamma+Z)$: the hydraulic grade line on the downstream side of the downstream orifice

H or $(p/\gamma+Z)$: the hydraulic grade line in the fuel rail after passage of injector pulse

H_I or $(p_I/\gamma+Z_I)$: the hydraulic grade line outside the injector orifice

For a given fuel rail, the pipeline impedance B is determined. With six independent equations and 10 variables, four of them can be arbitrarily specified. In a typical design, once the pipeline has been selected, as well as the required injector flow rate ΔQ, the designer is likely to identify the three external pressures. Then the remaining six variables H_o, H, Q_o, and the three orifice sizes are determined to provide a system free of terminal reflections. An instantaneous opening and closure of the injector needle is assumed as well as a time of opening less than the reflection time between injector and nearest terminal orifice. Should Q_o be one of the specified variables then one of the delivery pressures cannot be specified.

In the laboratory apparatus the injector orifice size and injector delivery pressure are fixed. With particular upstream and downstream orifices, only one operating condition exists to provide the reflectionless system. A number of tests are described in the next section to illustrate the behavior of the system with matched as well as with unmatched conditions.

5.0 EXPERIMENTAL AND NUMERICAL RESULTS

Procedure

A number of different experiments were performed with the important results given in this section. Numerical simulations for the given experimental conditions are also presented. The general procedure adopted for a given experiment was as follows;

A particular pulse width and frequency were selected and set with the injector controls. The choice of these was somewhat arbitrary; generally pulse widths were selected as 3, 5 or 8 msec and frequencies of 20 - 35 Hz for the injector operation were used.

A given flow condition was then set by installing particular orifices at the upstream and downstream ends of the line and adjusting system pressures to obtain the required flow condition. The upstream pressure was controlled by adjustment of the pump vane setting while the downstream pressure was established by an adjustable regulator.

The steady flow rate through the system was then measured as was the flow with the injector in operation. This was done by weighing a sample of fluid passed through the system in a given amount of time. The flow rate through the injector in its operating condition was also measured.

The experimental conditions were noted and a Polaroid photograph of the repeating oscilloscope trace was obtained. The oscilloscope scale factors were also noted.

Laminar Flows Results

The majority of the experiments were designed such that the steady flow (without injector operation) through the system was laminar. This was originally intended to provide a verification of the unsteady friction effects as discussed earlier in this report. The orifices were those originally supplied by Bendix (.0275 in. diameter downstream, .0362 in. diameter upstream). One experimental run and corresponding numerical simulation are given in Fig. 5.1. This particular result is to demonstrate a flow in which the matched impedance condition was not satisfied. This should not be interpreted as a typical flow result since different conditions could show a significantly different pressure trace. It is included to show the pressure fluctuations remaining in the system after the initial pressure pulse has propagated to the ends. A different flow condition with the same orifices but which did satisfy the matched impedance criteria is presented in Fig. 5.2. Although there are some residual pressure fluctuations after the initial pulse has passed the transducers, these are very small in magnitude and no systematic deviations are apparent. The numerical simulation shows essentially the same result. The deviations that are apparent are associated with the leading and trailing edges of the injector pulse where the flow rate is intermediate between the two matched conditions.

Additional experiments were performed by changing orifice diameters and establishing the new matched impedance conditions. These results are given in Fig. 5.3 and again show the validity of the concept as only very minor pressure fluctuations occur after the passage of the initial pressure wave.

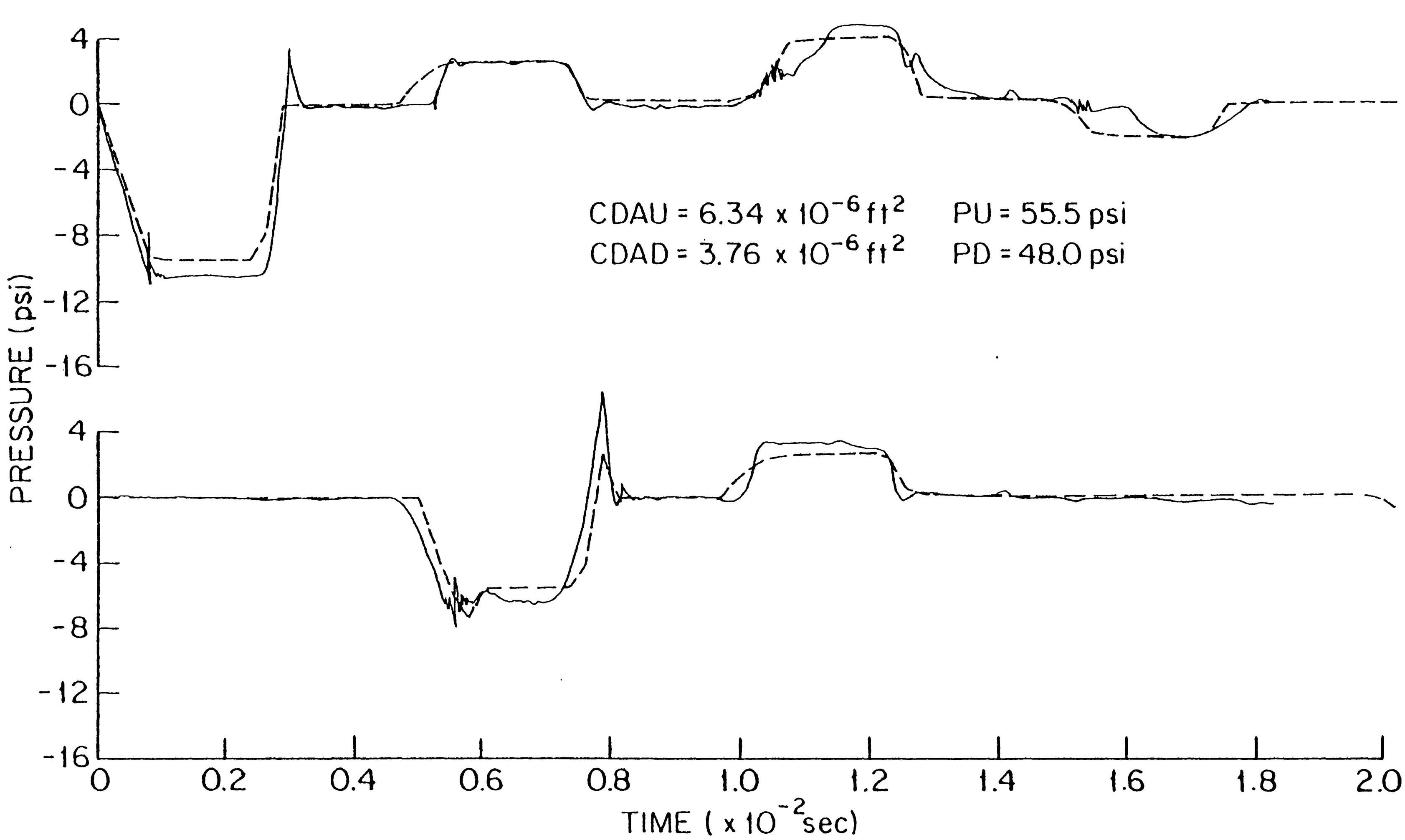

Fig. 5.1. Unmatched impedances, laminar flow.

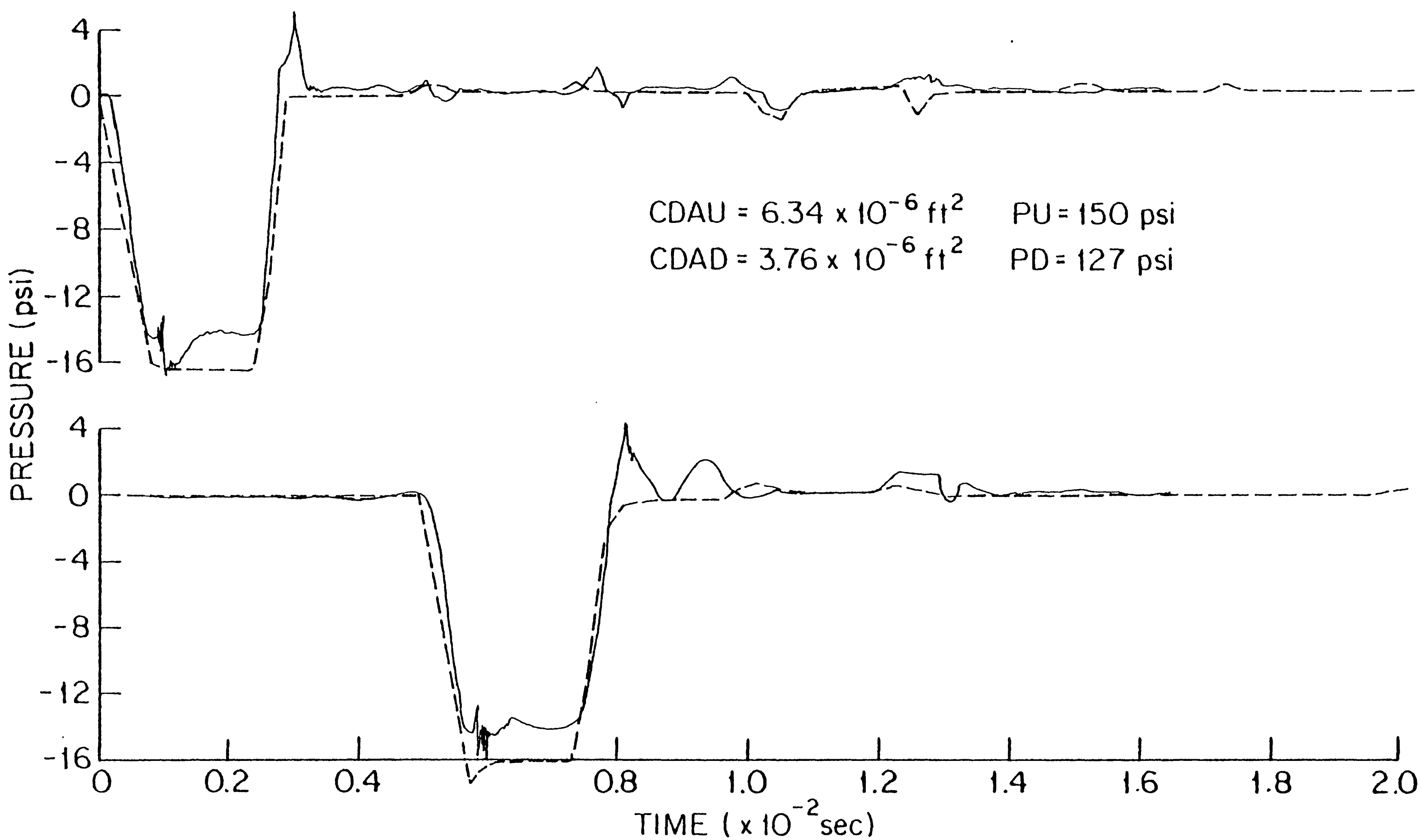

Figure 5.2. Matched impedances, laminar flow

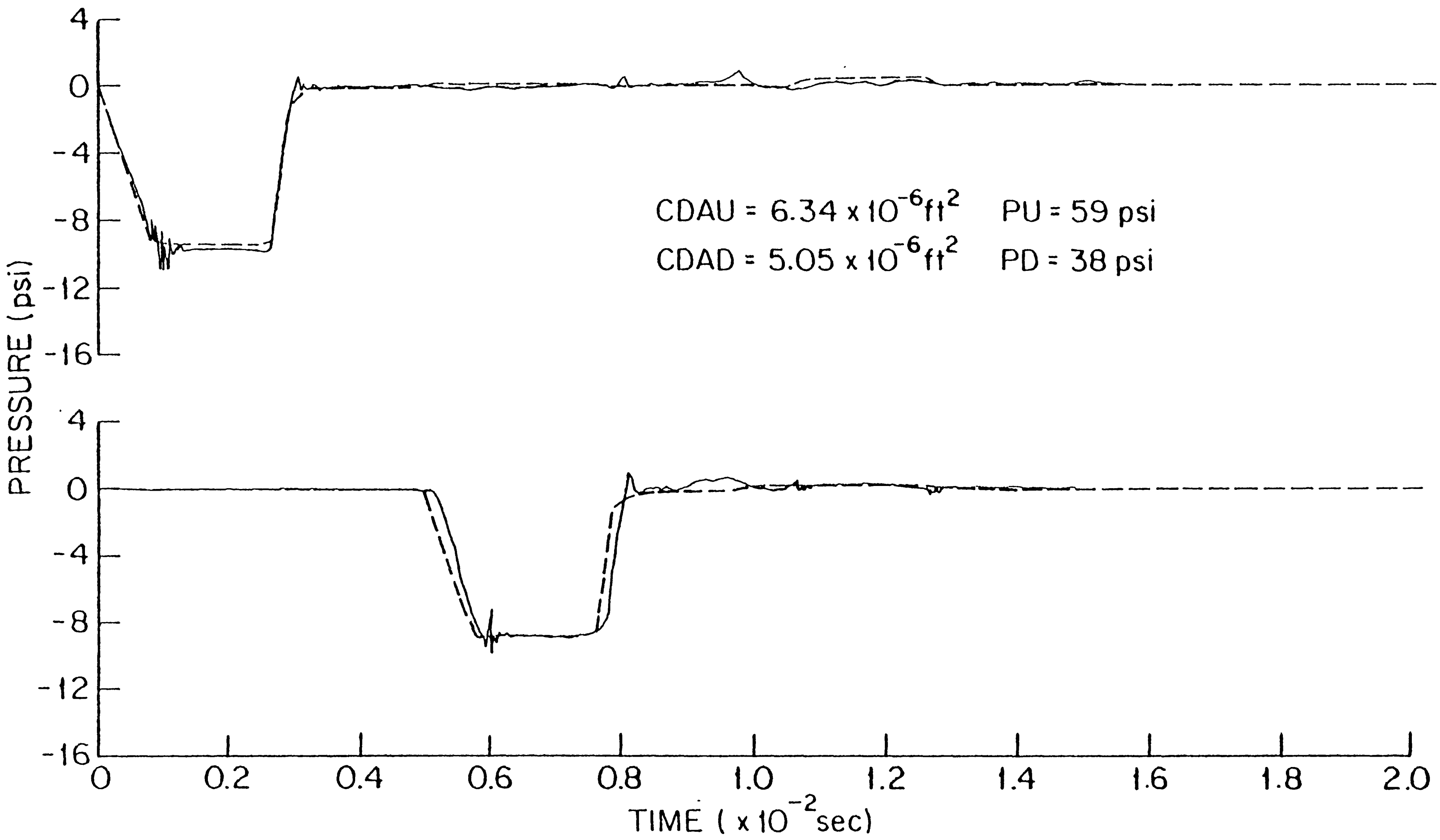

Fig. 5.3. Matched Impedances, laminar flow with different orifice.

Turbulent Flow

Two additional orifices (0.061 and 0.060 inch diameter) were supplied by Bendix and were intended to provide a flow condition in which the steady state flow through the system was turbulent at the matched impedance condition. However after the discharge coefficients were measured for the two orifices ($C_DA = 1.59 \times 10^{-5}$ ft^2 and 1.71×10^{-5} ft^2 for the 0.060 and 0.061 inch orifices respectively) the computed matched impedance condition required a higher pressure than the pump could supply. The numerical simulation of the matched impedance condition is presented, however, in Fig. 5.4, and shows a similar behavior to the results for laminar flow. In addition, new orifices were obtained so that the matched impedance conditions could be produced experimentally. This condition is given in Fig. 5.5 and indicates the validity of the concept for turbulent flows as well. Fig. 5.6 present an experiment where the matched impedance condition is not satisfied. Again, this result is for comparison purposes only and does not represent a general result for all flow conditions.

Additional Experiments.

Experiments were also performed to examine the necessity of the accumulators in the system. The flow condition considered was the same as that given in Fig. 5.3 with an accumulator and a regulator at both ends of the experimental system. The upstream regulator was added to the system for these particular tests. The experiment was then repeated with these devices progressively removed in the following order with the results presented in Figs. 5.7-5.12:

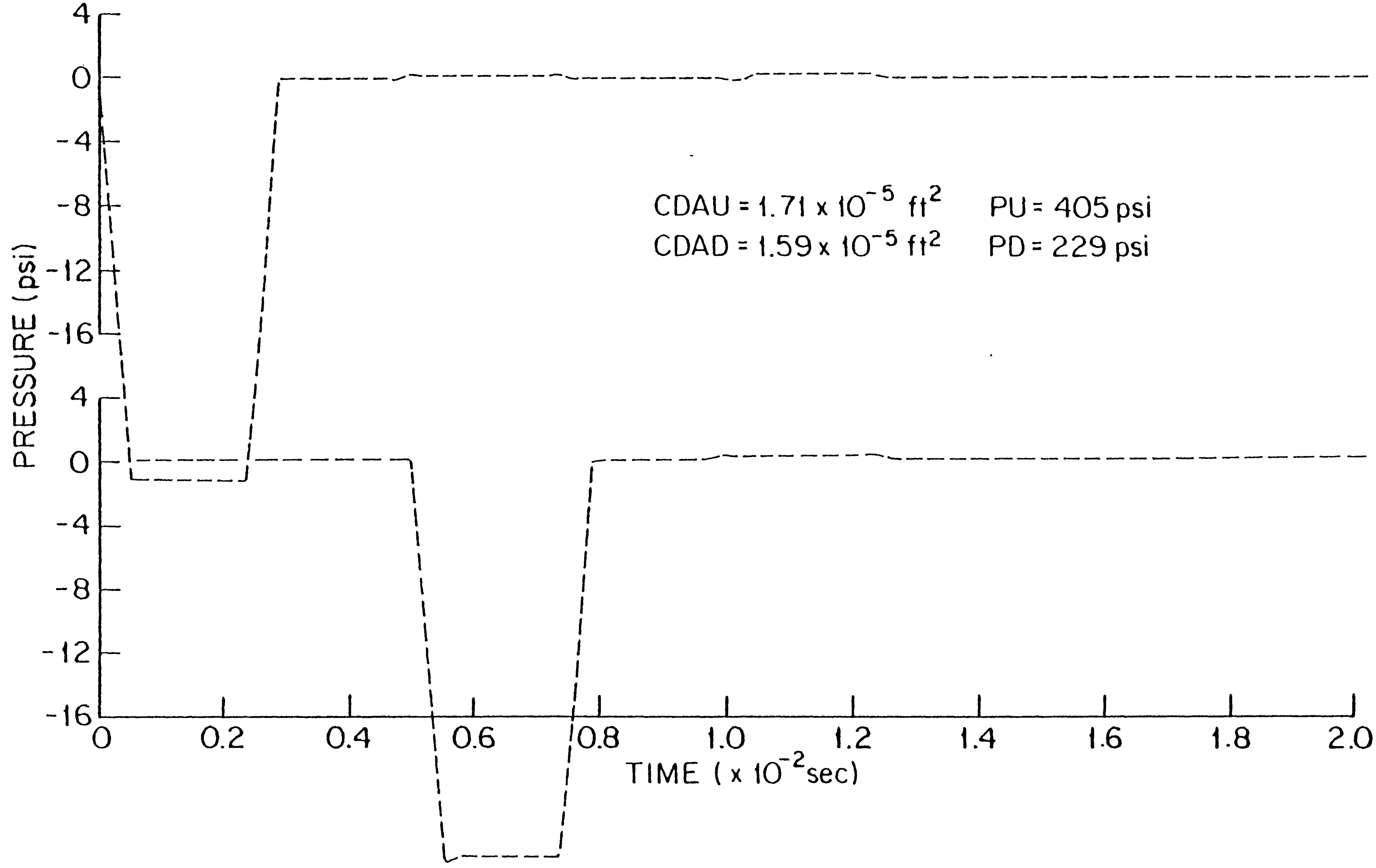

Fig. 5.4. Matched impedances, Turbulent flow, numerical simulation only.

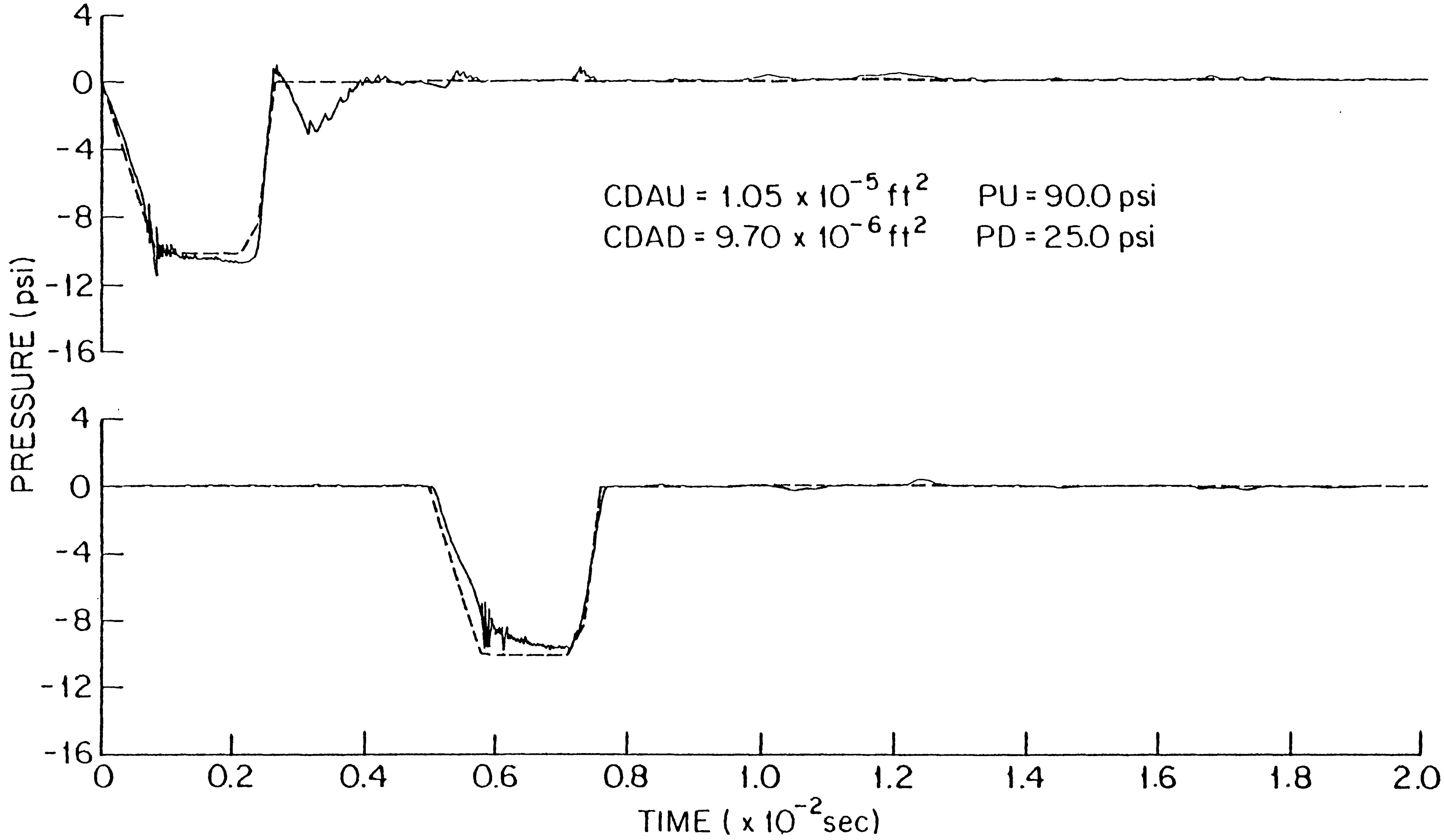

Fig. 5.5. Matched impedances, turbulent flow.

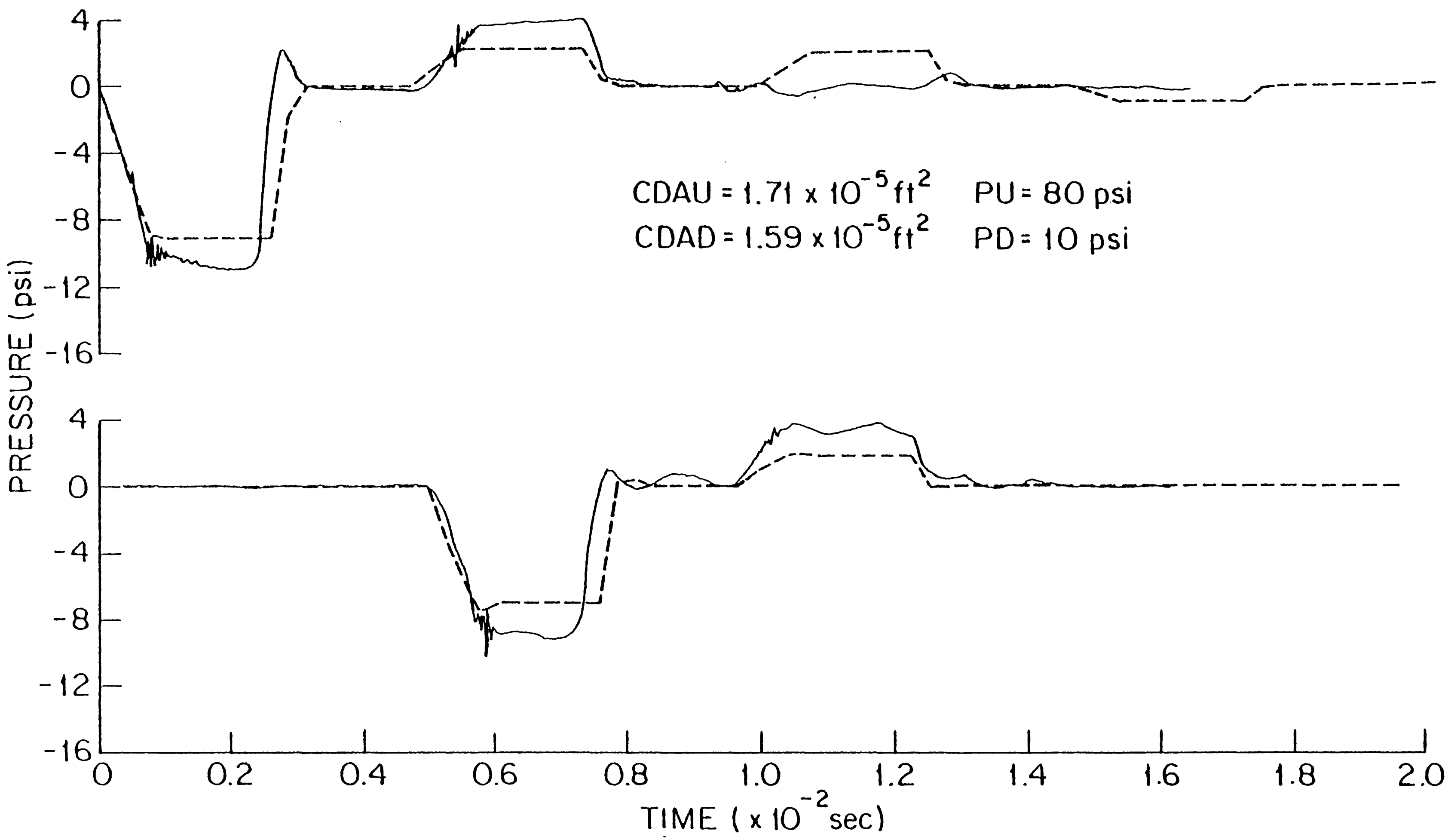

Fig. 5.6. Unmatched Impedances, Turbulent Flow.

Fig. 5.7 accumulators and regulators at both ends of system

Fig. 5.8 upstream regulator removed

Fig. 5.9 upstream accumulator removed

Fig. 5.10 upstream accumulator and regulator removed

Fig. 5.11 downstream accumulator removed

Fig. 5.12 upstream and downstream accumulators removed

The downstream regulator could not be removed with the matched impedance condition reproduced.

The results of these experiments can be summarized as follows: The removal of the regulators does not appear to make any significant difference to the system response. This can be seen in the similarity of both Figs. 5.6 and 5.7 and also Figs. 5.9 and 5.10. Each set of experiments is similar except that the upstream regulator has been removed in the second test. The removal of the accumulators appears to make a minor but detectable difference in response. The magnitude of pressure fluctuations increases by approximately 1-2 psi when the accumulators are removed but tends to be damped out after approximately one reflection and scarcely detectable afterward.

Pressure and Discharge Relations

An additional objective of the experimental study was to evaluate the potential for using the relationship in Eq. 4.1 in conjunction with measuring the pressure to determine the volume injected in a particular injection sequence. The volume injected ΔV is given as

$$\Delta V = \int 2\Delta Q \, dt = \frac{2}{B} \int (H_o - H)\, dt$$

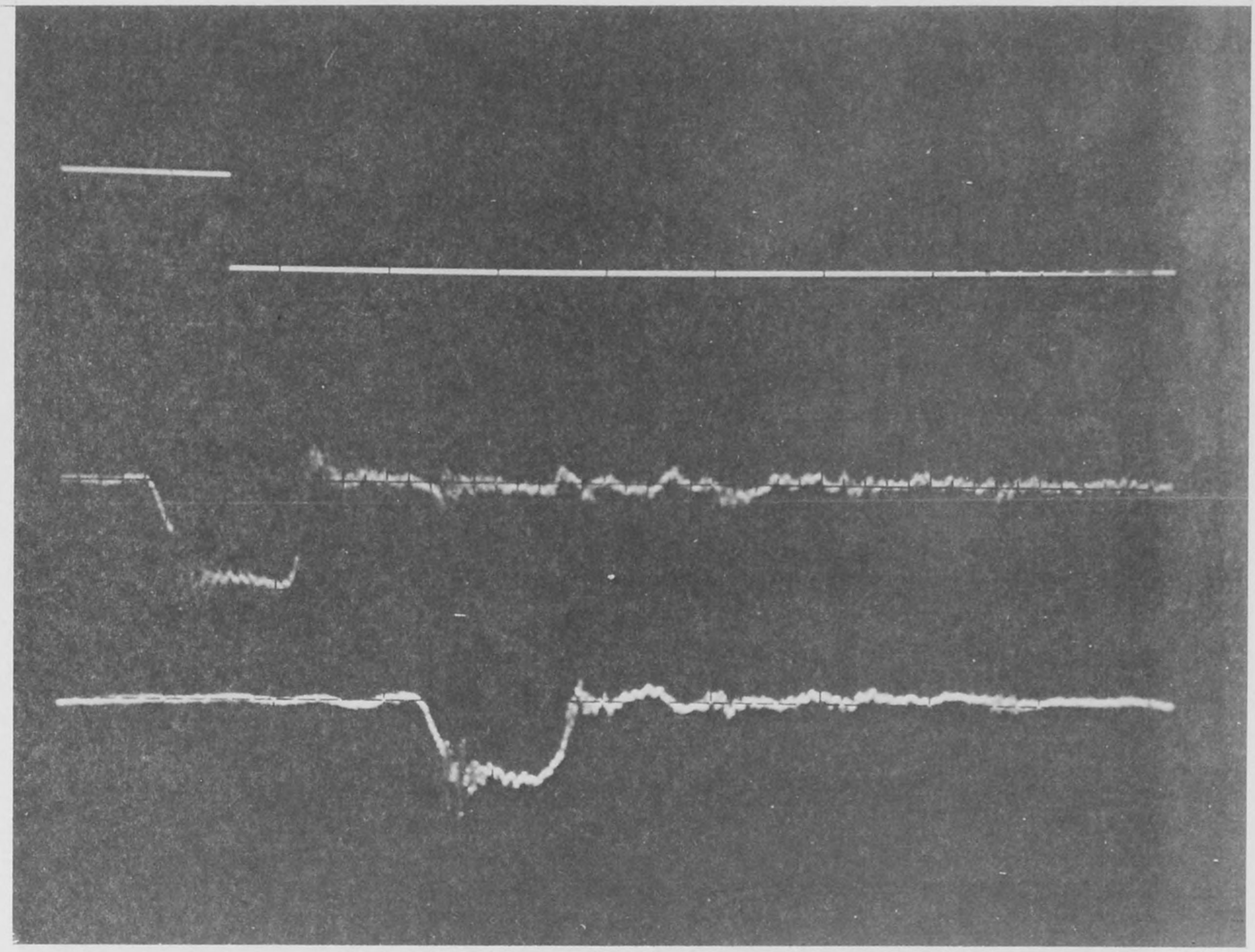

Fig. 5.7. All regulators and accumulators in system.

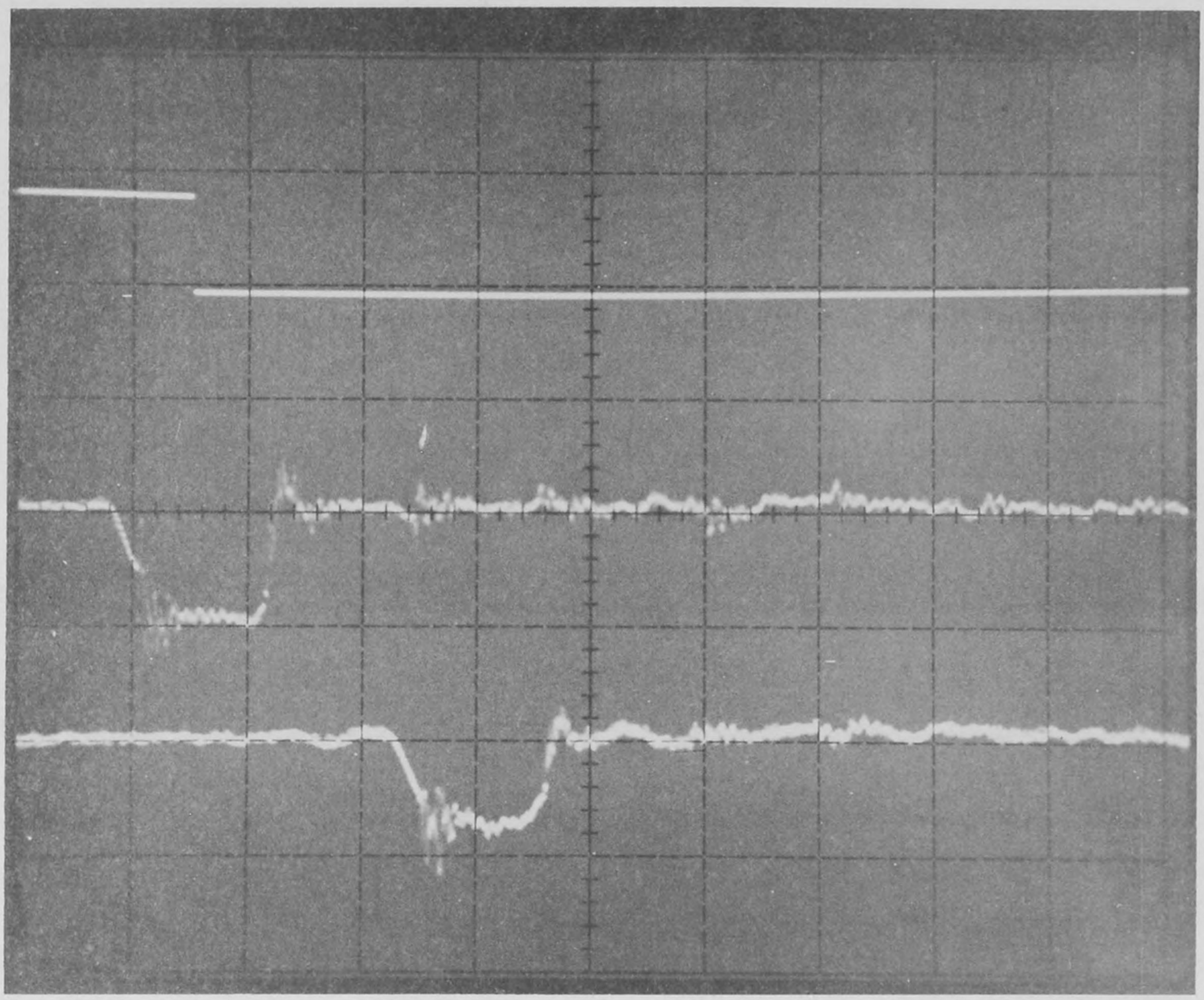

Fig. 5.8. Upstream regulator removed.

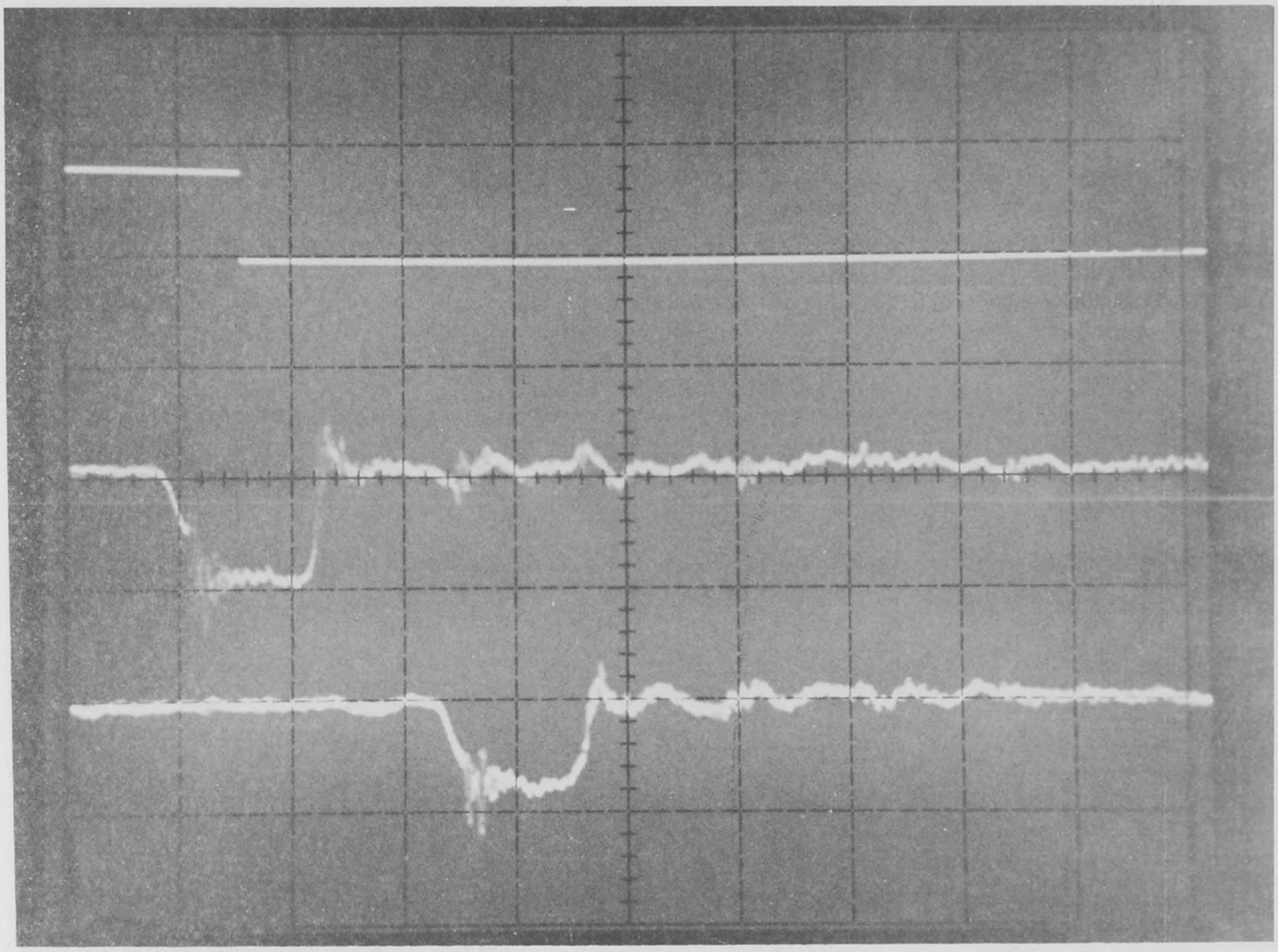

Fig. 5.9. Upstream accumulator removed

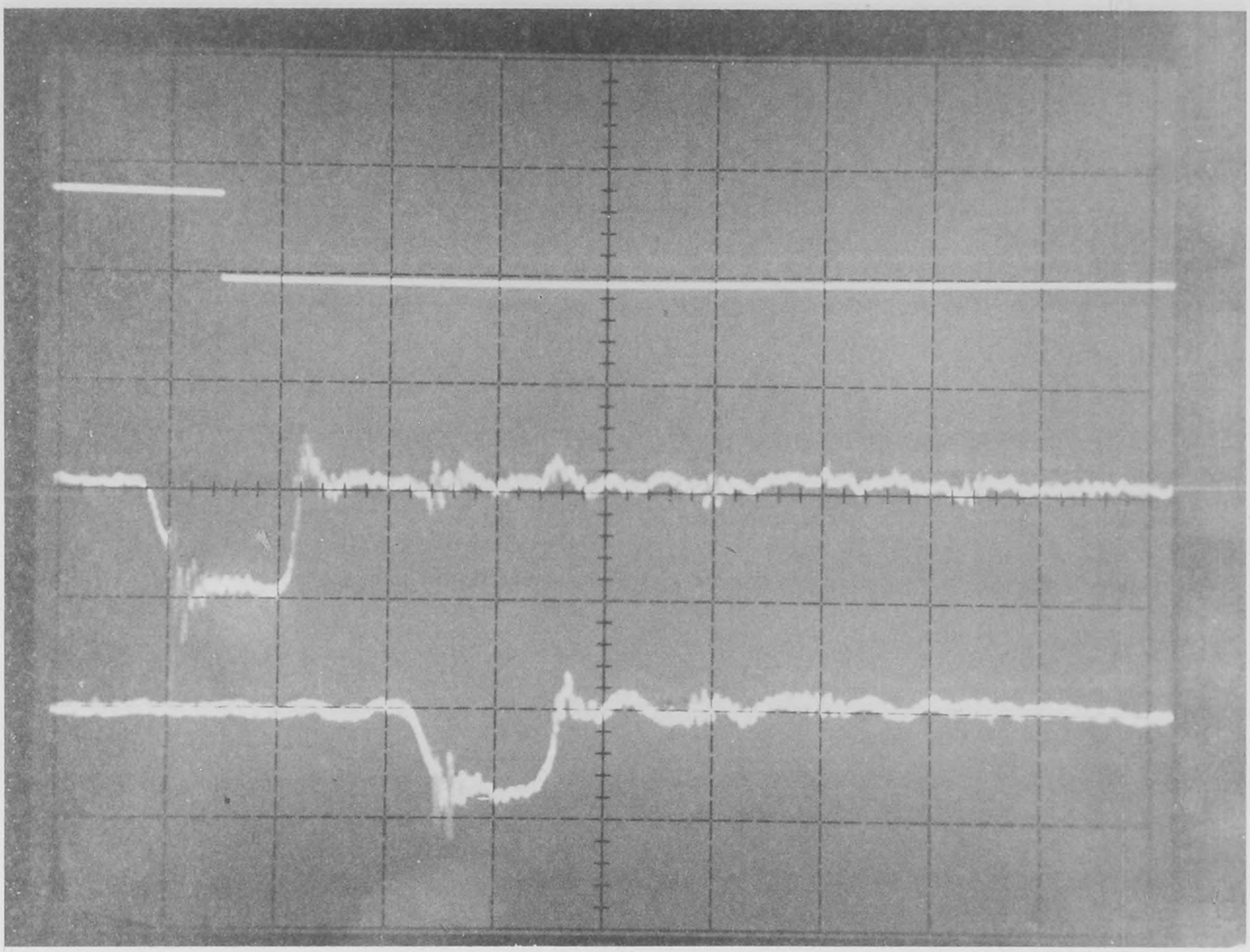

Fig. 5.10. Upstream regulator and accumulator removed.

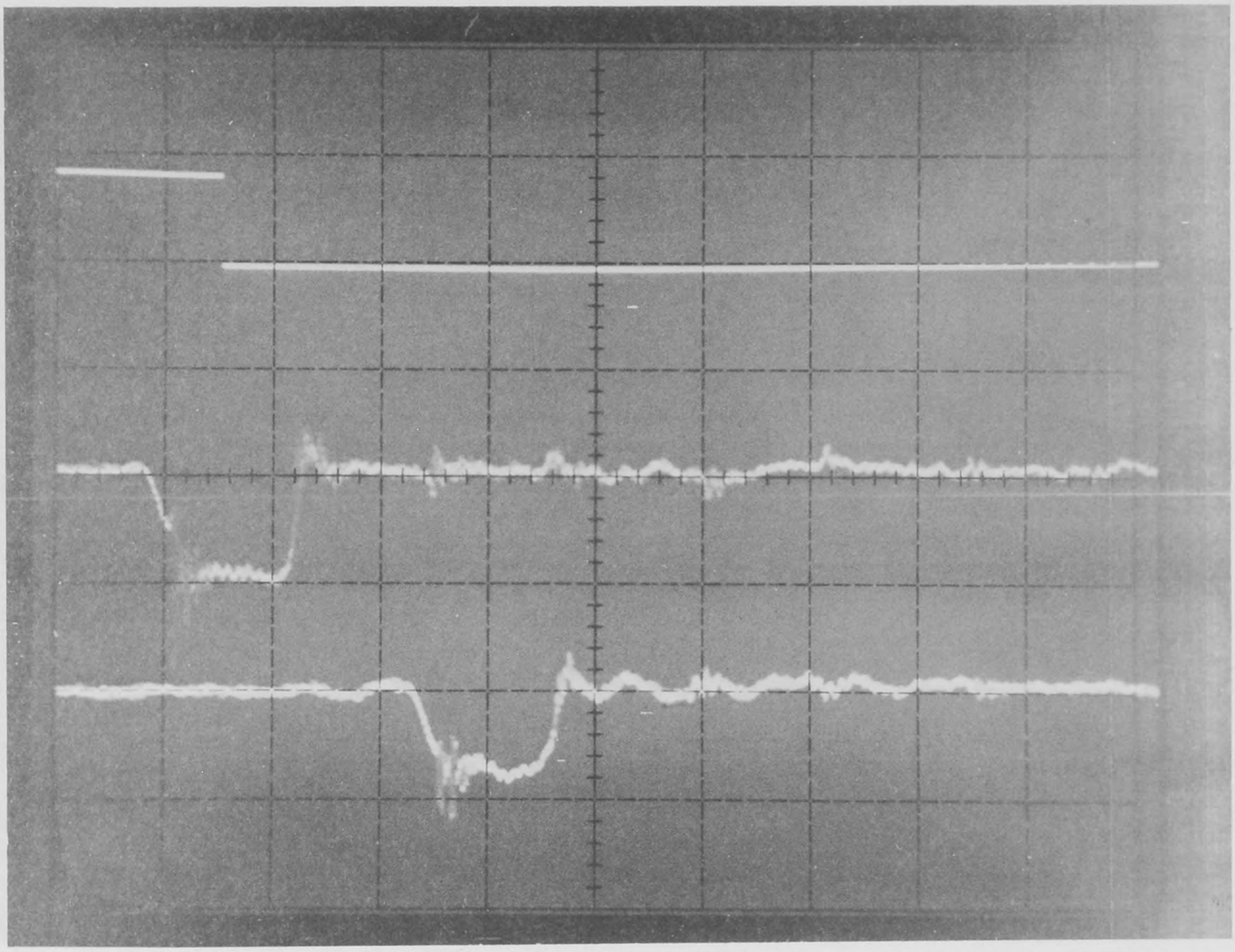

Fig. 5.11. Downstream accumulator removed.

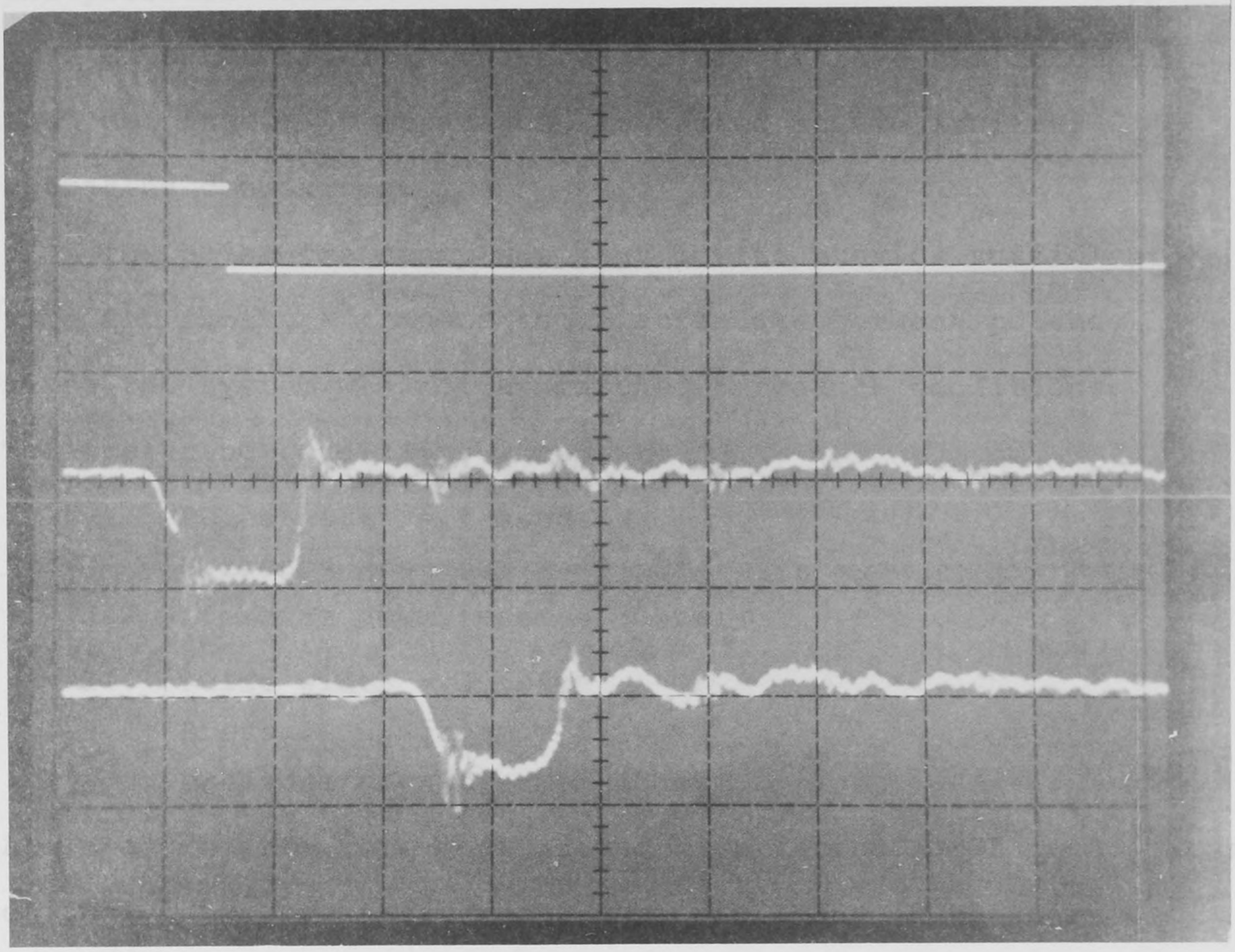

Fig. 5.12. Both accumulators removed.

The volume of fluid can thus be determined directly from the pressure trace.

Experiments were conducted to demonstrate the concept. The fuel injection apparatus was tested at two arbitrary operating conditions.

The pulse frequency was kept low to provide sufficient time for pressure transients to attenuate between pulses, since the system was not at matched impedance conditions. The operating conditions were:

I. Pulse width = 4 msec
Pressure upstream = 40 psi
Pressure downstream = 30 psi

II. Pulse width = 3 msec
Pressure upstream = 55 psi
Pressure downstream = 45 psi

All measurements were made at one time including 25 photographs of individual pressure traces for case I and 30 photographs for case II. Actual pulse volumes were measured by counting a given number of pulses and weighing the fluid mass associated with them. The average volume per pulse was computed from repeated measurements and determined to be accurate within $\pm$ 0.5% from the various measurements.

The area above the pressure drop trace was measured with a planimeter to evaluate the pressure-time integral. Figure 5.13 shows an image of several pressure traces which was used to select a procedure to measure the areas in a consistent manner. Interpretation of the area enclosed was as follows:

- Extrapolate a horizontal line across the top from the horizontal portion of the trace at the upper left. (ignore the small bump 2 squares from the left side).
- Extend a vertical line down from where the trace ends as one proceeds from far left to right.
- Extend a vertical line up from the trace where it ends as one proceeds from center to right.
- Pass a line through the center of the oscillations at the bottom of the photo, extrapolating horizontally to the left where information is missing.

These interpretations of the area are supported by reference to Fig. 5.13 which has recorded the high frequency noise at the beginning and end of the injector pulses.

Results of planimeter measurements of several photographs as given in Table 5.1 and corresponding photographs are given in Figs. 5.14 - 5.23. The remaining photographs were not analyzed. For the purposes of the calculations, the following conditions were used:

specific gravity of fluid = .76
wave speed = 3940 ft/sec
pipe diameter = .305 in

yielding a B value of 241160 sec/ft^2. The pressure transducer recording the pressure traces was taken to have a calibration factor of 1.055 psi/mv; a result of additional experiments beyond those discussed in Chapter 2. The possible error in each of the factors involved in each of the calculation parameters yielded an estimated maximum error of approximately $\pm$ 3-4%. All results in Table 5.1 are within this range and represent excellent agreement of the experiments with the theoretical concept.

Table 5.1 Experiments to compute volume Injected from Measured Pressure Trace.

Figure	Integrated Pressure (psi-msec)	Computed Volume ($ft^3 \times 10^{-7}$)	Measured Volume ($ft^3 \times 10^{-7}$)
5.14	26.12	6.58	6.505
5.15	26.10	6.57	"
5.16	26.25	6.61	"
5.17	26.29	6.62	"
5.18	26.25	6.61	"
5.19	22.92	5.77	5.87
5.20	23.14	5.82	"
5.21	22.90	5.76	"
5.22	23.26	5.86	"
5.23	22.95	5.78	"

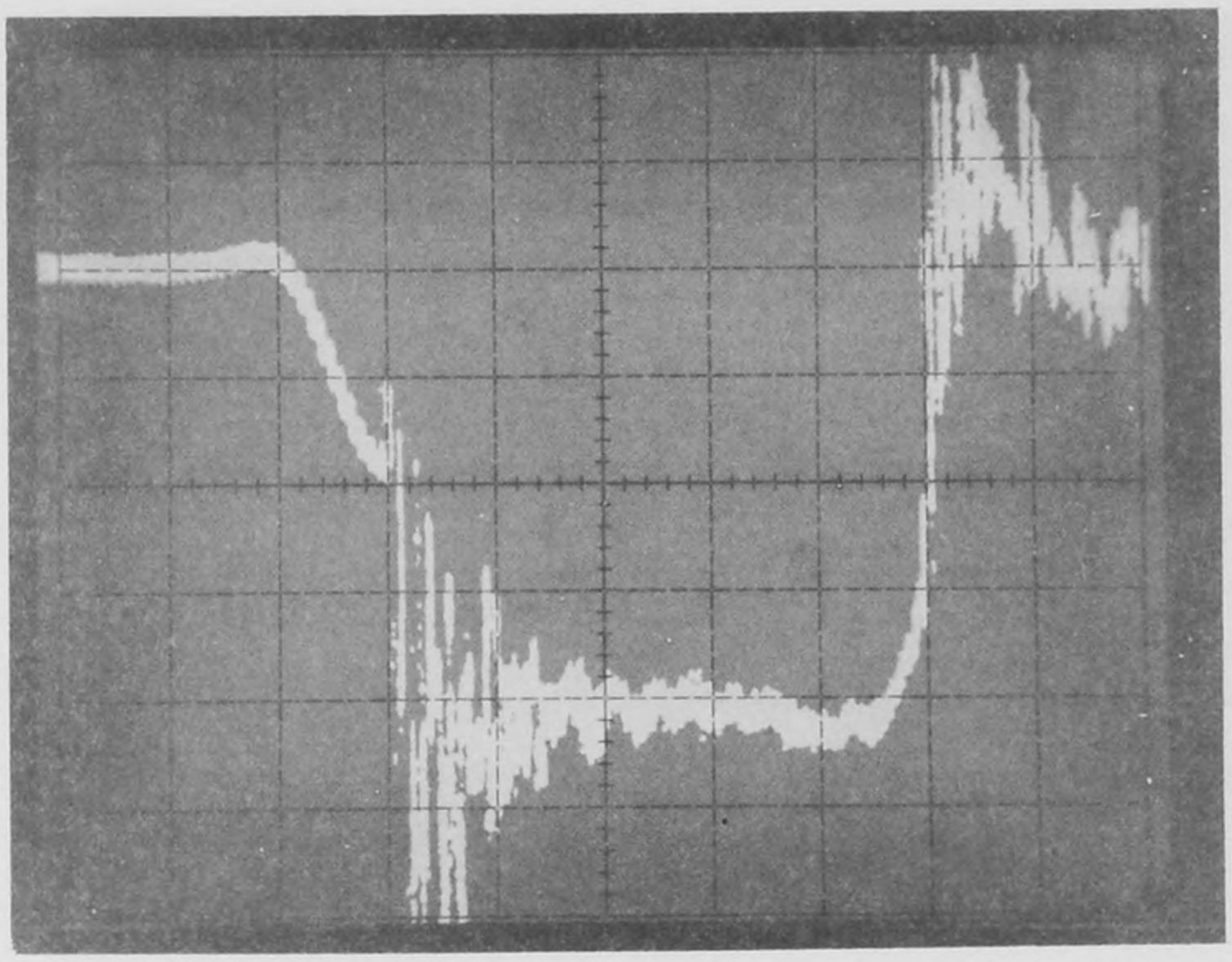

Fig 5.13 Composite photograph of several Case II injections

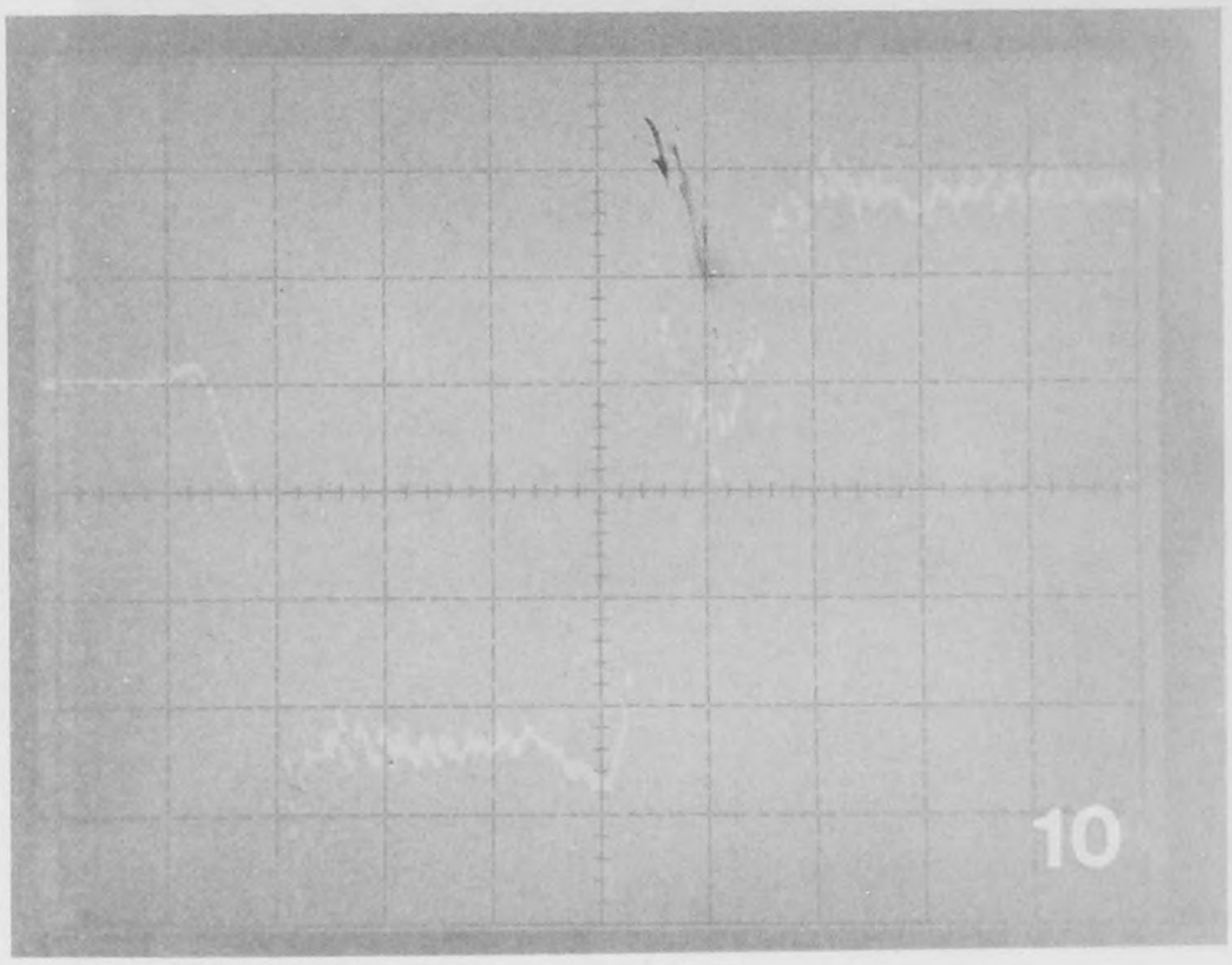

Fig 5.14 Case I

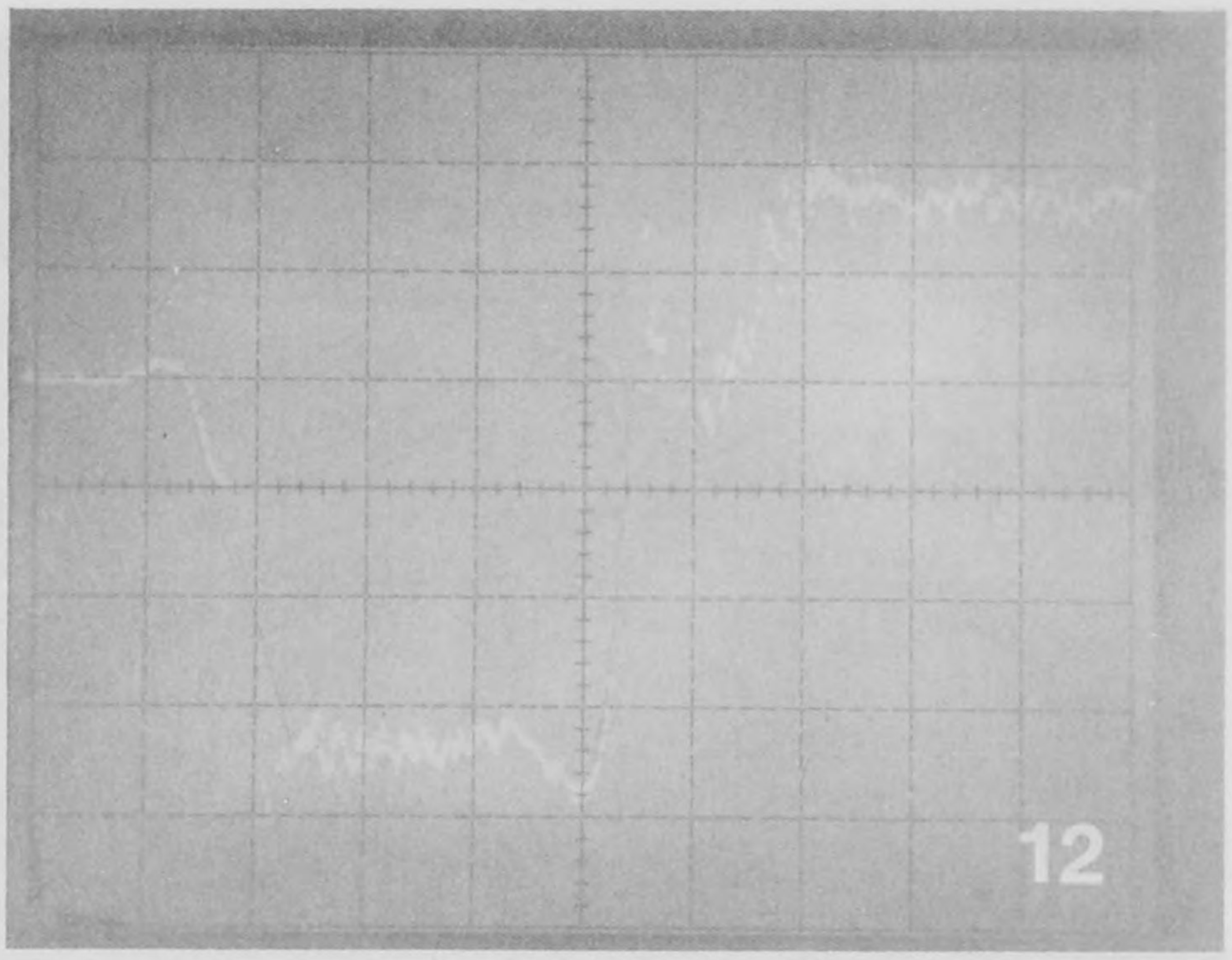

Fig 5.15 Case I

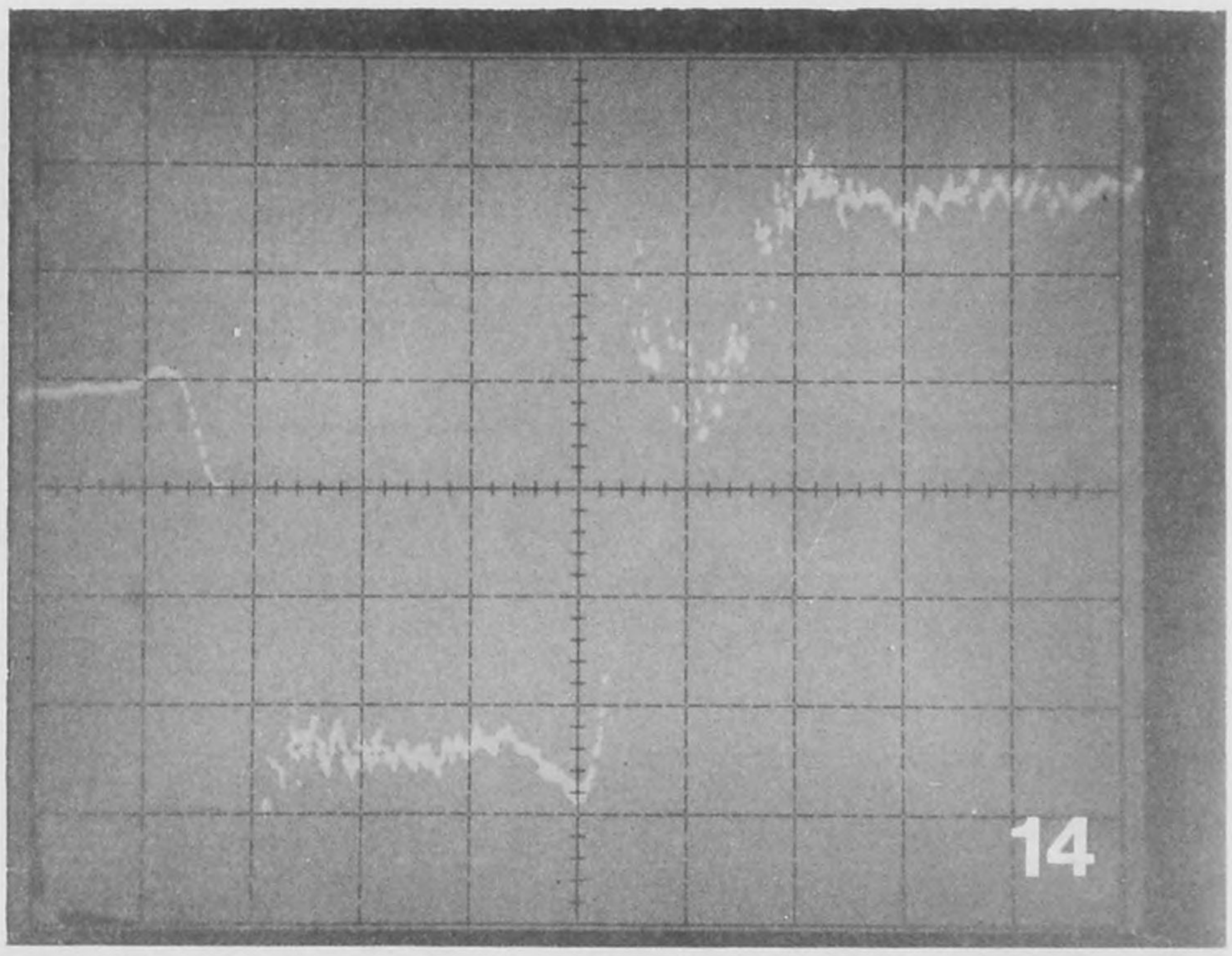

Fig 5.16 Case I

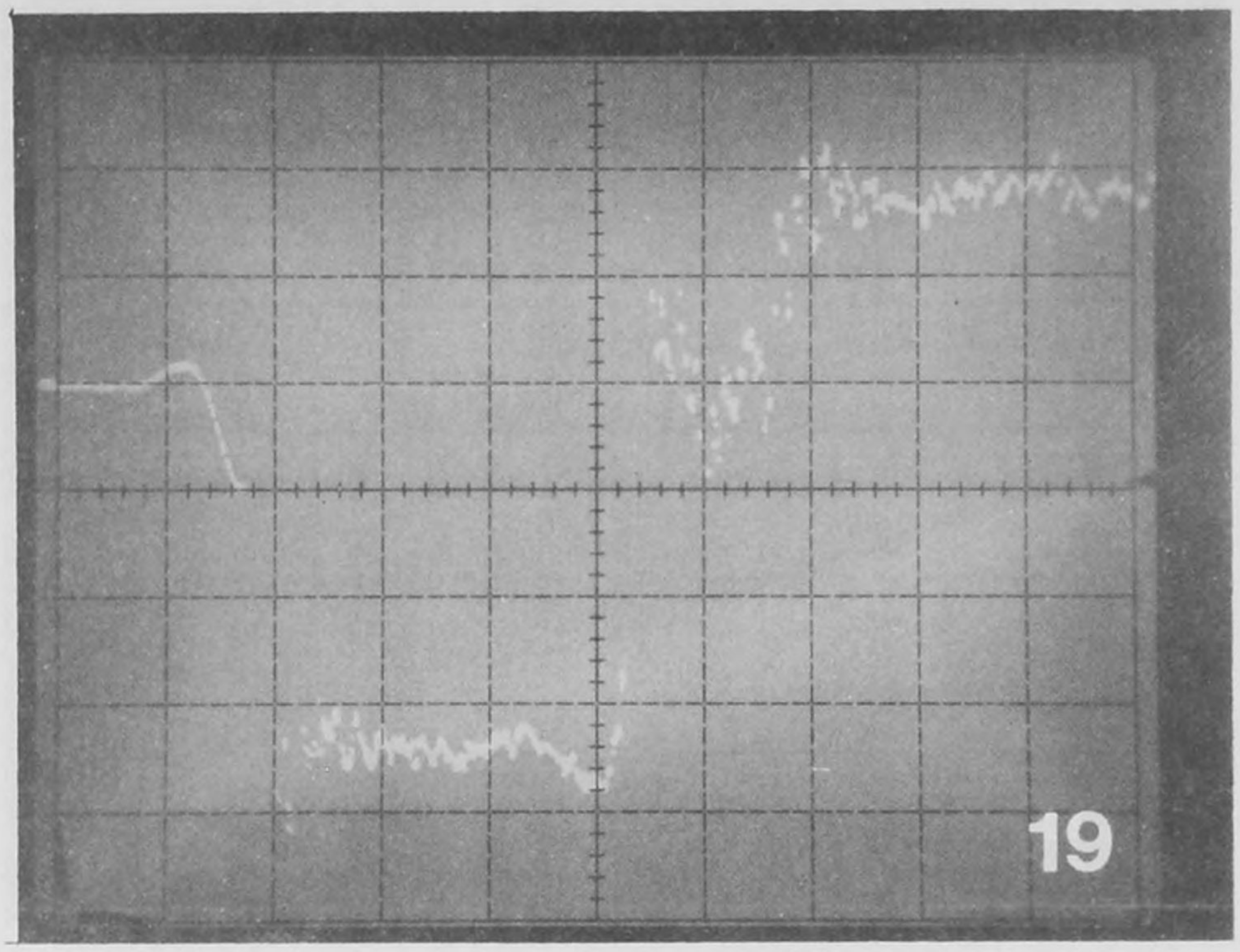

Fig 5.17 Case I

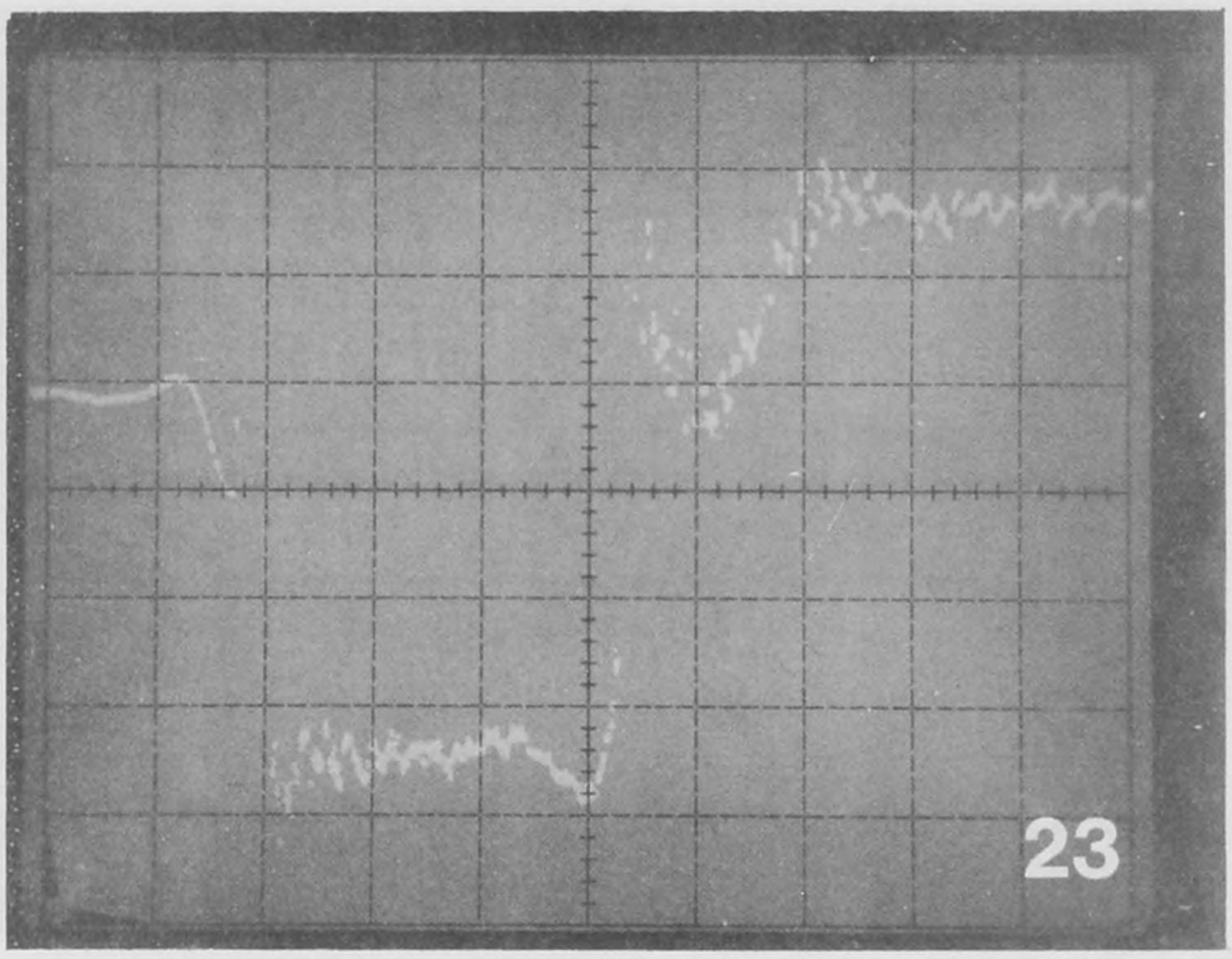

Fig 5.18 Case II

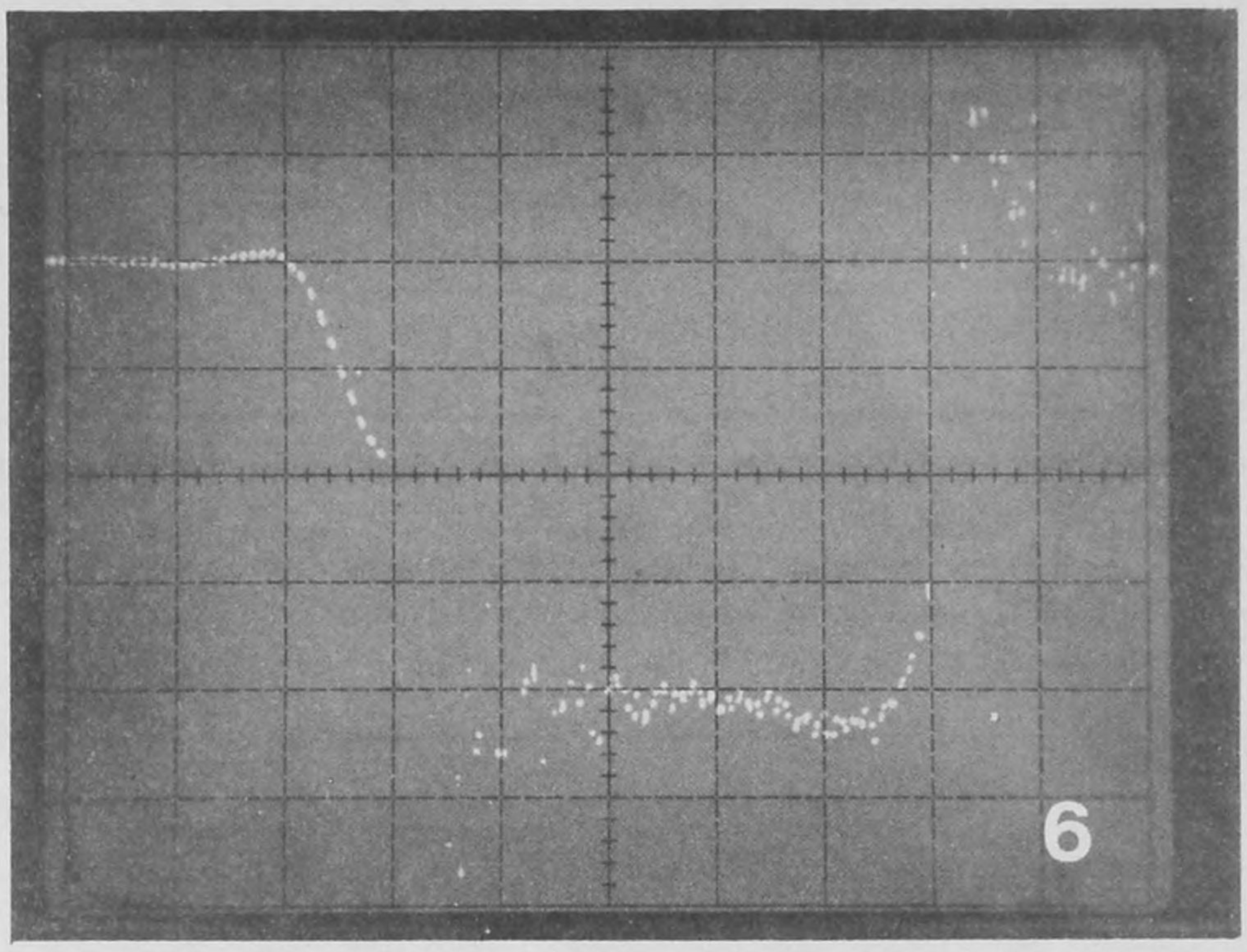

Fig 5.19 Case II

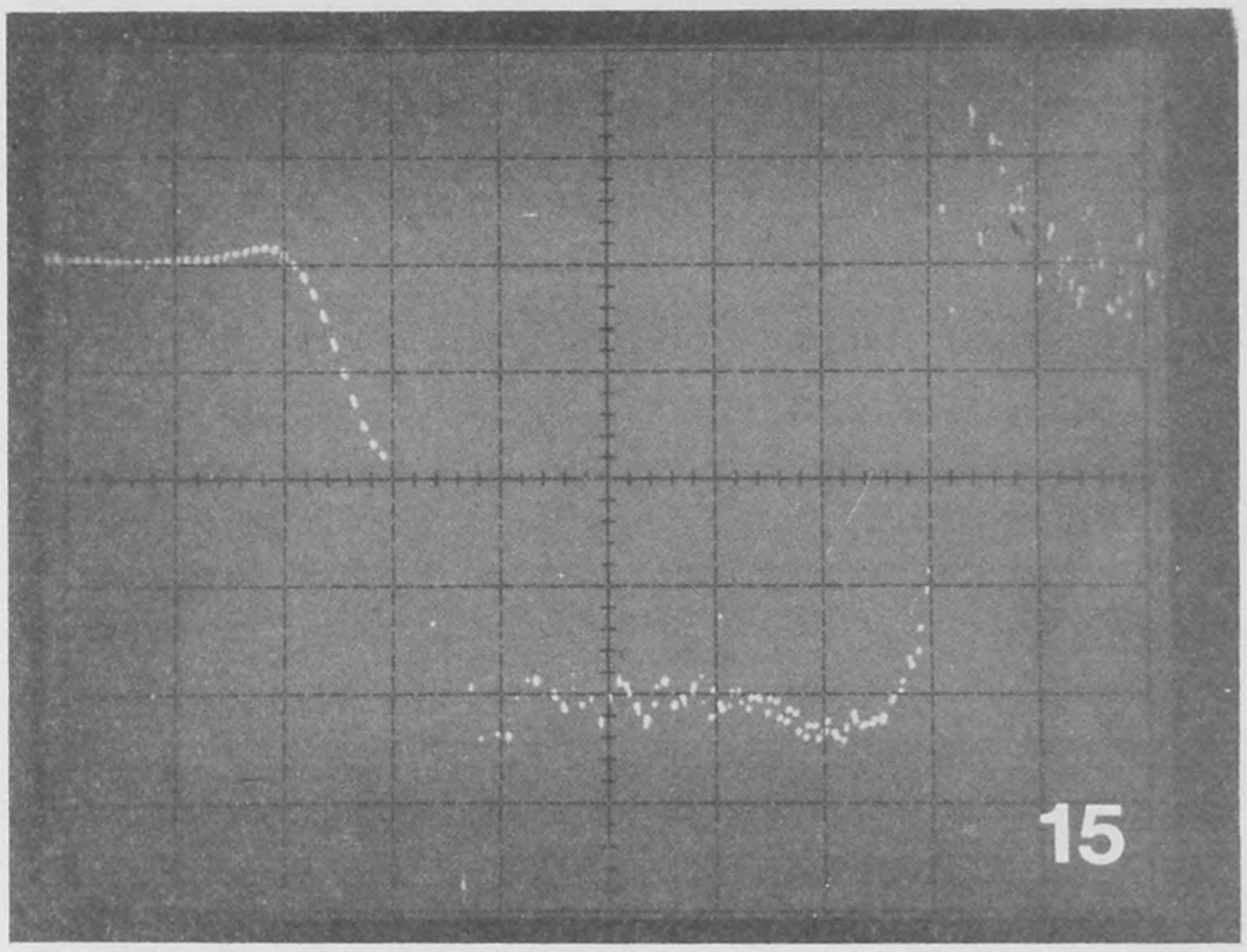

Fig 5.20 Case II

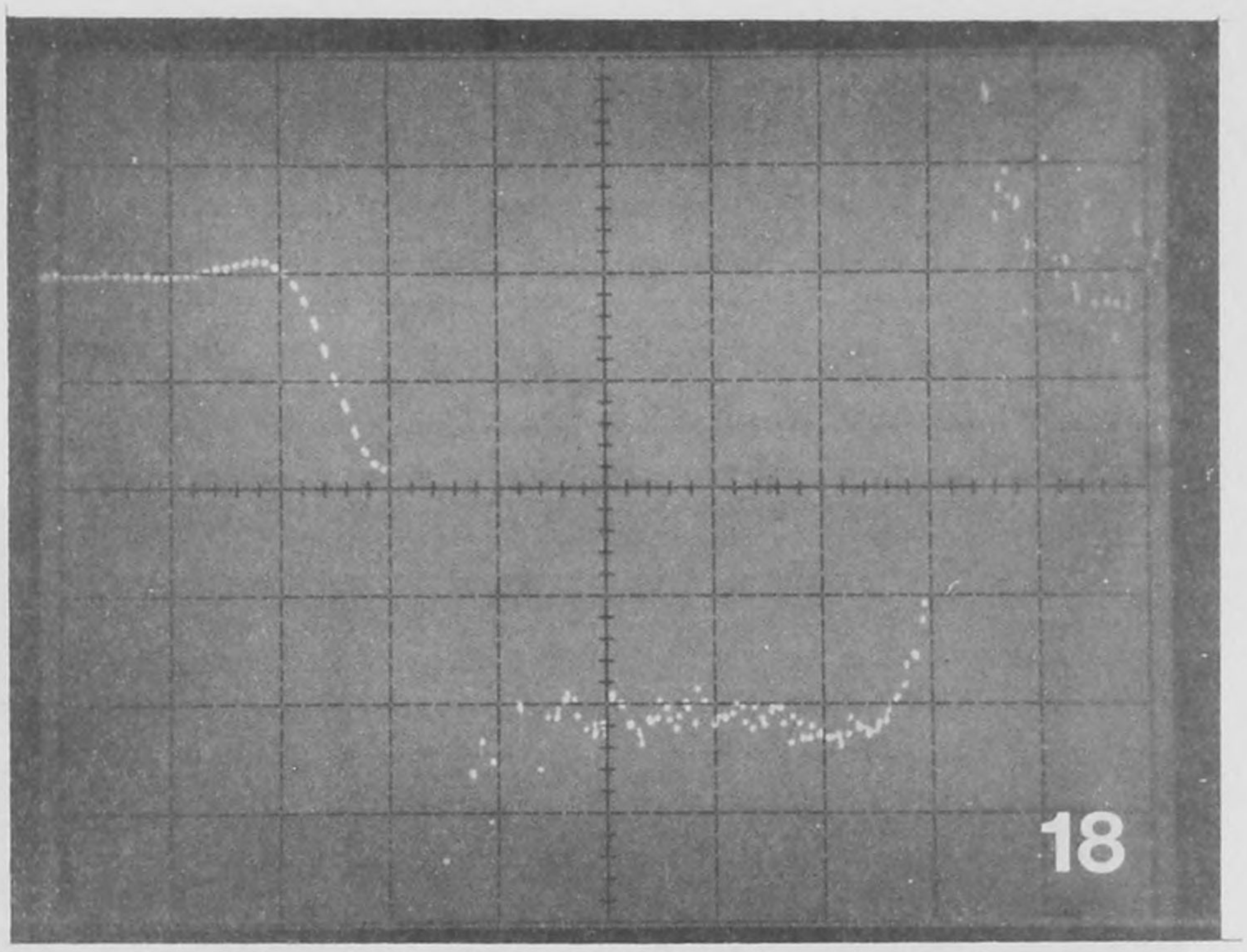

Fig 5.21 Case II

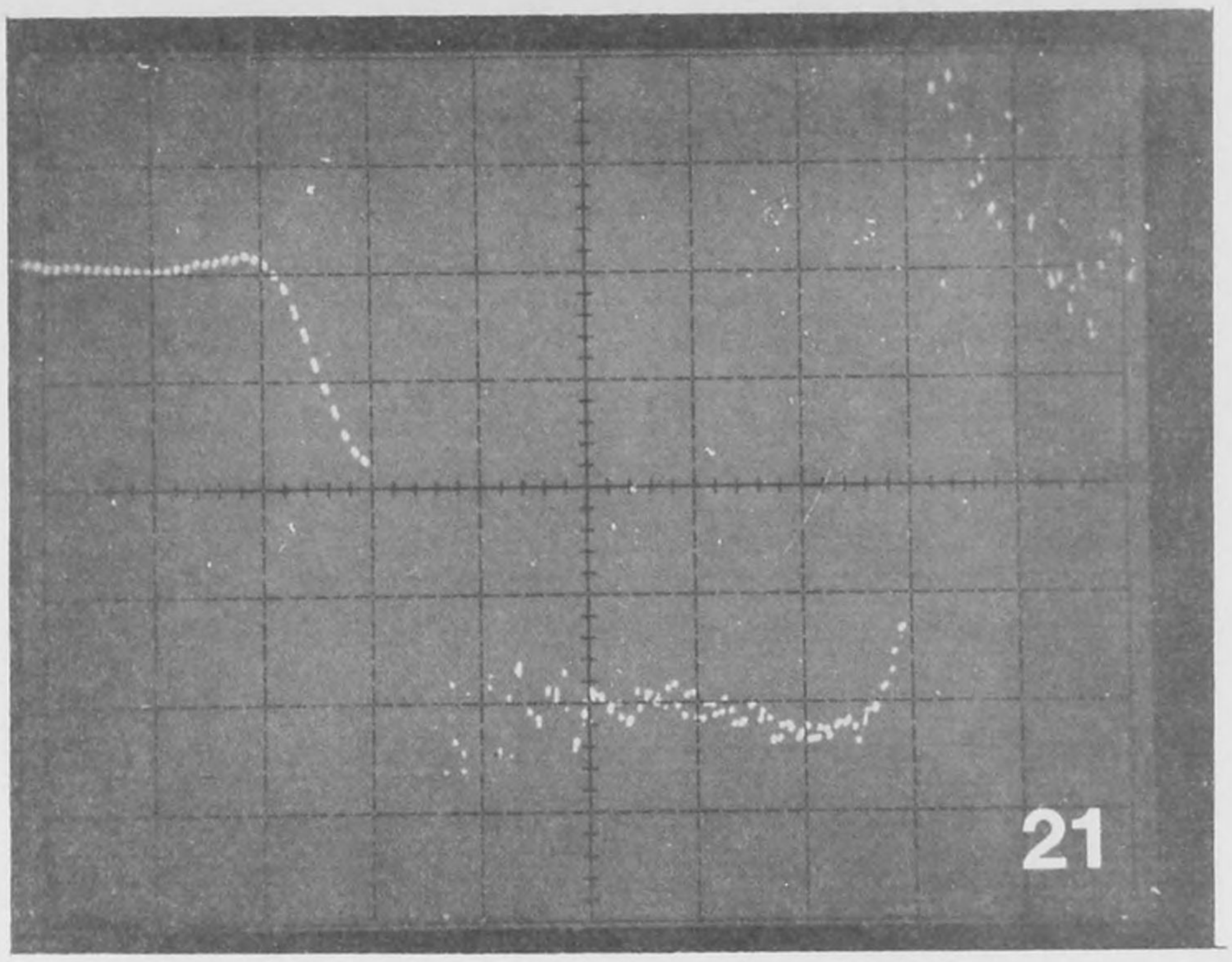

Fig 5.22 Case II

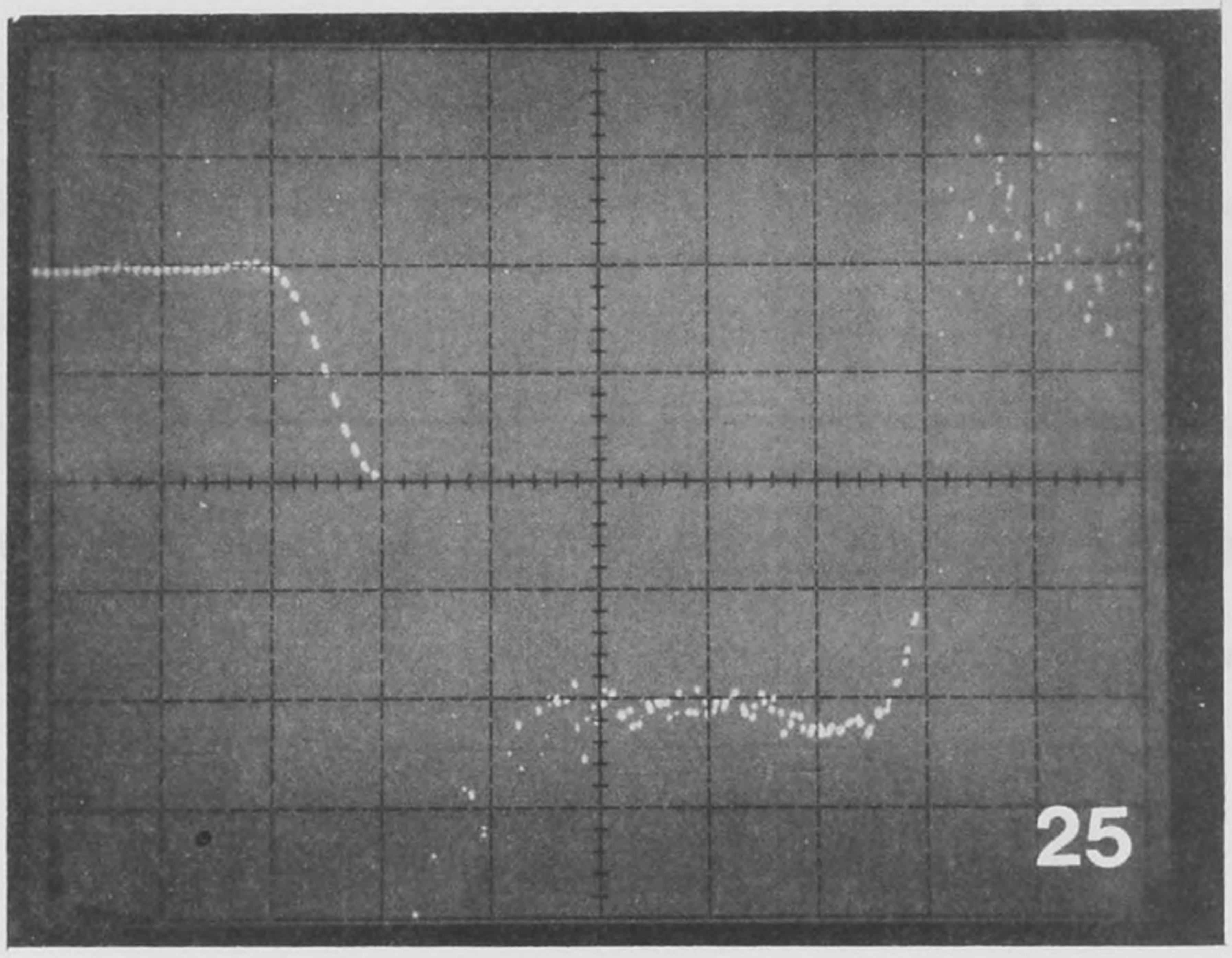

Fig 5.23 Case II

6.0 SUMMARY

The results of this study have demonstrated the concept of minimizing pressure fluctuations by applying the matched impedance principle to a fuel injection system. The results of the experimental investigations indicate that when the matched flow conditions are achieved, the pressure fluctuations remaining in the system after the initial response to fuel injector operation are not of practical importance. The experimental results were conducted for both laminar and turbulent flow systems. The computer model used to simulate the experimental data was found to be in good agreement, indicating that the numerical model can be a useful tool for predicting the major features of the system response for actual fuel injection systems.

The results also indicated that the unsteady friction influences on the flow behavior were negligible for the particular system. This was true because the major pressure drops in the system were in the orifices used to create the matched impedance conditions and so friction effects were negligible. Although the numerical model for laminar flow was developed with unsteady friction effects included, the results were not significantly different than if the instantaneous local velocities were used to compute friction losses. In the turbulent flow model, this latter approach was used, and the good agreement of the numerical simulations with experimental data indicate that unsteady influences were again minor.

Finally, the principle of the determination of the fuel volume injected by monitoring the pressure response of the fuel delivery system was demonstrated. By integrating the pressure response over time and applying the waterhammer relations, it was possible to compute the volume of fuel passed through the fuel injector. This principle has potential application to various flow control devices on an actual fuel injection system.

7.0 ACKNOWLEDGEMENTS

Mr. Dan Cooper ably performed most of the experimental work and carried out many of the numerical comparisons during this project.

The cooperation of Bendix personnel particularly Mr. Lael Taplin, in providing the experimental apparatus and for considerable technical interaction, is greatly appreciated.

APPENDIX A

FORTRAN program and output,
laminar flow with frequency
dependent friction.

```
C BENDIX FUEL INJECTION SYSTEM. RESERVOIR AND ORIFICE AT EACH PIPE END.
C FUEL INJECTOR AT INTERNAL SECTION.
C LAMINAR FRICTION, STAGGERED GRID. N MUST BE EVEN.
C INJECTOR AT SECTION NJS, WHICH MUST BE ODD.
C LAMINAR FREQUENCY DEPENDENT LOSSES, ZIELKE'S WEIGHTING FUNCTION.
C NUMBER OF TERMS IN FRICTION TERM IS KMAX.
      DIMENSION H(62),Q(62),EL(62),QF(62,91),W(91),HF(62),HFF(91)
     1,TAD(15),TD(15),TIME(200),PINJ(200),POS(200)
      NAMELIST/DIN/A,XL,D,G,EL,PU,PD,CDAU,CDAD,CDAI,PI,TMAX,N,IPR,VISC
     1,KMAX,RHO,PER,NDATA,TAD,TD,NJS,IDIAG,IPLT
   10 READ (5,DIN,END=220)
      IF(N/2*2.NE.N) N=N+1
      IF(KMAX/2*2.NE.KMAX) KMAX=KMAX+1
      KM1=KMAX+1
      NS=N+1
      NS2=NS+1
      AR=.7854*D*D
      FC=16.*VISC*XL/(G*D*D*AR*FLOAT(N))
      R=32.*VISC*XL/(FLOAT(N)*G*D*D*AR)
      B=A/(G*.7854*D*D)
      DT=XL/(A*FLOAT(N))
      GAM=RHO*G
      HU=EL(1)+PU/GAM
      HD=EL(NS)+PD/GAM
      HI=EL(NJS)+PI/GAM
      A1=.5/G*(1./CDAU**2+1./CDAD**2)
      CV=G*CDAU*CDAU
      CVD=G*CDAD*CDAD
      CI=CDAI*SQRT(2.*G)
      VCL=0.
C FIND STEADY STATE FLOW AND STORE INITIAL VARIABLES
      Q0=.5*(-R*N+SQRT(R*R*N*N+4.*A1*(HU-HD)))/A1
      H(1)=HU-Q0*Q0*.5/CV
      DO 20 I=1,NS2
      H(I)=H(1)-(I-1)*R*Q0
      Q(I)=Q0
      DO 20 KK=1,KM1
   20 QF(I,KK)=Q0
      QINJ=0.
      PP=GAM*(H(NJS)-EL(NJS))/144.
      PPP=GAM*(H(N)-EL(N))/144.
      CALL WEIGHT(W,DT,KMAX,VISC,D)
      WRITE(6,30) (W(I),I=1,KMAX)
   30 FORMAT(' W=',(10F7.3))
      T=0.
      TT=0.
      K=0
      WRITE (6,40) A,XL,D,VISC,PU,PD,PI,Q0,CDAU,CDAD,CDAI,G,TMAX,DT,B,N,
     1NJS,IPR,NDATA,RHO,PER,(TD(I),TAD(I),I=1,NDATA)
   40 FORMAT(' A,XL,D,VISC=',2F8.1,2E9.2/' PU,PD,PI,Q0=',3F8.2,E12.4/
     1' CDAU,CDAD,CDAI=',3E9.2/' G,TMAX, DT, B =',F8.3,2F8.4,F9.1/
     2' N, NJS,IPR,NDATA=',4I4/' RHO,PER,TD,TAD=',2F8.4/(2F8.5))
      WRITE(6,50)
   50 FORMAT('          P AND DISCHARGES ALONG THE PIPE'//
     1'    TIME X/L=       0.       INJ       1.       QINJ')
C BEGINNING OF TRANSIENT LOOP
   60 P1=(H(1)-EL(1))*GAM/144.
      P2=(H(NJS)-EL(NJS))*GAM/144.
      P3=(H(N)-EL(N))*GAM/144.
```

```
      Q1=Q(1)/Q0
      Q2=Q(NJS)/Q0
      Q3=Q(N)/Q0
      Q4=QINJ/Q0
      WRITE(6,70) T,P1,P2,P3,Q1,Q2,Q3,Q4
   70 FORMAT (1H ,F8.5,4H  P=,3F9.3,/10X,3H Q=,4F9.3)
   80 L=K/2+1
      TIME(L)=T
      PINJ(L)=GAM/144.*(H(NJS)-EL(NJS))-PP+24.
      PDS(L)=GAM/144.*(H(N)-EL(N))-PPP
      IF (T.GT.TMAX) GO TO 10
C  REPOSITION VELOCITIES IN STORAGE AND EVALUATE VISCOUS LOSSES AT
C SECTION.
      II=2
      III=1
   90 DO 110 I=III,NS,2
      DO 100 KK=1,KMAX
  100 QF(I,KK)=QF(I,KK+1)
      QF(I,KMAX+1)=Q(I)
      HF(I)=R*Q(I)
      DO 110 KK=1,KMAX
      KF=KMAX+2-KK
      A1=FC*(QF(I,KF)-QF(I,KF-1))*W(KK)
      HF(I)=HF(I)+A1
  110 IF(I.EQ.N) HFF(KK)=A1
      IF(III.EQ.2)GOTO 140
      DO 120 KK=1,KMAX
  120 QF(NS2,KK)=QF(NS2,KK+1)
      QF(NS2,KMAX+1)=Q(NS2)
      HF(NS2)=R*Q(NS2)
      DO 130 KK=1,KMAX
      KF=KMAX+2-KK
      A1=FC*(QF(NS2,KF)-QF(NS2,KF-1))*W(KK)
  130 HF(NS2)=HF(NS2)+A1
  140 IF(III.EQ.1)GO TO 160
      HB=R*Q(N)
      HP=HF(N)-HB
      IF(IDIAG.EQ.1)WRITE(6,150)HB,HP,HF(N),(KK,HFF(KK),KK=1,KMAX)
  150 FORMAT(' HB,HP,HF(N)=',3F10.5/(1X,10(I3,F7.3)))
  160 K=K+1
      T=T+DT
C COMPUTATION OF INTERIOR POINTS
      DO 180 I=II,N,2
      IF(I.EQ.NJS) GO TO 180
      CP=H(I-1)+Q(I-1)*B-HF(I-1)
      QX=Q(I+1)
      HX=HF(I+1)
      IF(I+1.NE.NJS)GO TO 170
      QX=Q(NS2)
      HX=HF(NS2)
  170 CM=H(I+1)-QX*B+HX
      H(I)=.5*(CP+CM)
      Q(I)=(H(I)-CM)/B
  180 CONTINUE
      IF (II.EQ.3) GO TO 190
      III=2
      II=3
      GO TO 90
C UPSTREAM BOUNDARY
  190 CM=H(2)-Q(2)*B+HF(2)
```

```
          S=1.
          IF(HU-CM.LT.0.)S=-1.
          Q(1)=S*(-CV*B+SQRT(CV*B*CV*B+S*2.*CV*(HU-CM)))
          H(1)=CM+B*Q(1)
C DOWNSTREAM BOUNDARY
          CP=H(N)+Q(N)*B-HF(N)
          S=1.
          IF(CP-HD.LT.0.)S=-1.
          Q(NS)=S*(-CVD*B+SQRT(CVD*CVD*B*B+S*2.*CVD*(CP-HD)))
          H(NS)=CP-B*Q(NS)
C INJECTOR BOUNDARY
C FIND INJECTOR FLOW
          TT=TT+DT*2./PER
          IF(TT.GT.1.) TT=TT-1.
          DO 200 I=2,NDATA
          KK=I-1
          IF(TD(I).GT.TT) GO TO 210
    200 CONTINUE
    210 TA=TAD(KK)+(TT-TD(KK))*(TAD(KK+1)-TAD(KK))/
       1(TD(KK+1)-TD(KK))
          CP=H(NJS-1)+Q(NJS-1)*B-HF(NJS-1)
          CM=H(NJS+1)-Q(NJS+1)*B+HF(NJS+1)
          A1=CP+CM+(B*CI*TA*.5)**2
          H(NJS)=.5*(A1-SQRT(A1*A1-(CP+CM)**2-(B*CI*TA)**2*HI))
          Q(NJS)=(-CM+H(NJS))/B
          Q(NS2)=(CP-H(NJS))/B
          QIO=QINJ
          QINJ=Q(NS2)-Q(NJS)
          VOL=VOL+DT*(QIO+QINJ)
          IF(TA.EQ.1.) QMAX=QINJ
          IF(K/IPR*IPR-K) 80,60,80
    220 QAVE=VOL/PER
          WRITE(6,230) VOL,QAVE,QMAX
    230 FORMAT(' VOLUME INJECTED PER CYCLE=',F12.9/
       1' AVERAGE FLOW RATE OVER CYCLE=',F12.8/
       2' MAX FLOW RATE AT INJECTOR=',F12.8)
          IF(IPLT.EQ.1) CALL PLOT(TIME,PINJ,PDS,L,0.,-14.,.002,8.,10.,7.)
          STOP
          END
                SUBROUTINE WEIGHT(W,DT,KMAX,VISC,D)
C WEIGHT EVALUATES THE WEIGHTING FUNCTION FOR SPECIFIC VALUES OF TAU.
          DIMENSION W(1)
          TAU1=VISC*4./(D*D)
          DO 20 K=1,KMAX
          TAU=TAU1*(2*K-1)*DT
          ST=SQRT(TAU)
          IF(TAU.GT..02) GO TO 10
          W(K)=.282095/ST-1.25+1.057855*ST+.9375*TAU+.396696*TAU*ST-
         1.351563*TAU*TAU
          GO TO 20
     10 W(K)=1./EXP(26.3744*TAU)+1./EXP(70.8493*TAU)+1./EXP(135.0198*TAU)
        1+1./EXP(218.9216*TAU)+1./EXP(322.5544*TAU)
     20 CONTINUE
          RETURN
          END
 &DIN XL=29.2,A=4000.,D=.025417,G=32.2,EL=2*0.,60*3.28,
 CDAI=2.6E-6,PI=0.,
 PU=8568.,PD=5357.,RHO=1.5,CDAU=6.34E-6,CDAD=5.05E-6,VISC=1.26E-5,
 TMAX=.0053,N=56,NJS=19,IPR=2,KMAX=30,NDATA=5,IDIAG=0,IPLT=0,
 PER=.05,TAD=0.,1.,1.,0.,0.,TD=0.,.014,.05,.055,1., &END
```

```
W= 87.211 49.827 38.317 32.193 28.246 25.432 23.296 21.603 20.218 19.059
18.069 17.211 16.459 15.792 15.195 14.657 14.168 13.722 13.313 12.936
12.587 12.262 11.960 11.677 11.411 11.161 10.926 10.703 10.493 10.293
A,XL,D,VISC=  4000.0    29.2 0.25E-01 0.13E-04
PU,PD,PI,QO= 8563.00 5357.00    0.00  0.2514E-03
CDAU,CDAD,CDAI= 0.63E-05 0.51E-05 0.26E-05
G,TMAX, DT, B =  32.200  0.0053  0.0001 244830.1
N, NJS,IPR,NDATA=  56  19   2   5
PHC,PER,TD,TAD=  1.5000  0.0500
0.00000 0.00000
0.01400 1.00000
0.05000 1.00000
0.05500 0.00000
1.00000 0.00000
      P AND DISCHARGES ALONG THE PIPE
   TIME X/L=        0.         INJ        1.         QINJ
 0.00000  P=     51.308    50.177    50.115
          Q=      1.000     1.000     1.000      0.000
 0.00026  P=     51.308    46.424    50.115
          Q=      1.000     0.818     1.000      0.364
 0.00052  P=     51.308    42.943    50.115
          Q=      1.000     0.650     1.000      0.699
 0.00078  P=     51.308    40.705    50.115
          Q=      1.000     0.543     1.000      0.914
 0.00104  P=     51.308    40.686    50.115
          Q=      1.000     0.543     1.000      0.914
 0.00130  P=     51.308    40.672    50.115
          Q=      1.000     0.543     1.000      0.914
 0.00156  P=     51.308    40.661    50.115
          Q=      1.000     0.543     1.000      0.914
 0.00182  P=     51.308    40.650    50.115
          Q=      1.000     0.543     1.000      0.914
 0.00209  P=     51.308    40.641    50.115
          Q=      1.000     0.543     1.000      0.913
 0.00235  P=     51.308    40.632    50.115
          Q=      1.000     0.543     1.000      0.913
 0.00261  P=     47.931    44.419    50.115
          Q=      1.188     0.727     1.000      0.546
 0.00287  P=     44.505    50.058    50.114
          Q=      1.353     1.000     1.000      0.000
 0.00313  P=     42.169    50.079    50.114
          Q=      1.454     1.000     1.000      0.000
 0.00339  P=     42.104    50.089    50.114
          Q=      1.457     1.000     1.000      0.000
 0.00365  P=     42.073    50.096    50.114
          Q=      1.459     1.000     1.000      0.000
 0.00391  P=     42.053    50.102    50.114
          Q=      1.459     1.000     1.000      0.000
 0.00417  P=     42.038    50.106    50.114
          Q=      1.460     1.000     1.000      0.000
 0.00443  P=     42.026    50.110    50.114
          Q=      1.460     1.000     1.000      0.000
 0.00469  P=     42.015    50.113    50.114
          Q=      1.461     1.000     1.000      0.000
 0.00495  P=     45.841    50.364    50.114
          Q=      1.291     1.012     1.000      0.000
 0.00521  P=     51.096    50.363    46.605
          Q=      1.013     1.012     0.830      0.000
 0.00547  P=     51.183    50.260    43.003
          Q=      1.008     1.007     0.680      0.000
VOLUME INJECTED PER CYCLE= 0.000000525
AVERAGE FLOW RATE OVER CYCLE=  0.00001049
MAX FLOW RATE AT INJECTOR=  0.00022964
```

APPENDIX B
FORTRAN program and output, turbulent flow

```
C BENDIX FUEL INJECTION SYSTEM. RESERVOIR AND ORIFICE AT EACH PIPE END.
C FUEL INJECTOR AT INTERNAL SECTION.
C TURBULENT FRICTION, STAGGERED GRID. N MUST BE EVEN
C INJECTOR AT SECTION NJS, WHICH MUST BE ODD.
C COLEBROOK FORMULA TO EVALUATE FRICTION FACTOR
C HEAD LOSS EVALUATED IN SUBROUTINE HF
      DIMENSION H(62),Q(62),EL(62),TAD(15),TD(15),TIME(200),
     1PINJ(200),PDS(200)
      NAMELIST/DIN/A,XL,D,G,EL,PU,PD,PI,CDAU,CDAD,CDAI,TMAX,N,IPR,VISC
     1,RHO,PER,NDATA,TAD,TD,NJS,EPS,IPLT
   10 READ (5,DIN,END=150)
      IF(N/2*2.NE.N)N=N+1
      NS=N+1
      NS2=NS+1
      DX=XL/ (N)
      AR=.7854*D*D
      B=A/(G*.7854*D*D)
      DT=XL/(A* (N))
      GAM=RHO*G
      HU=EL(1)+PU/GAM
      HD=EL(NS)+PD/GAM
      HI=EL(NJS)+PI/GAM
      CV=G*CDAU*CDAU
      CVD=G*CDAD*CDAD
      CI=CDAI*SQRT(2.*G)
      VOL=0.
      A1=0.5/CV+0.5/CVD
C FIND STEADY STATE FLOW AND STORE INITIAL VARIABLES
      Q0=SQRT((HU-HD)/A1)
      DO 20 I=1,5
      R=HF(Q0,D,AR,VISC,EPS,DX,G)/Q0/Q0
   20 Q0=SQRT((HU-HD)/(A1+R*FLOAT(N)))
      H(1)=HU-Q0*Q0*.5/CV
      DO 30 I=1,NS2
      H(I)=H(1)-(I-1)*R*Q0*Q0
   30 Q(I)=Q0
      H(NS2)=H(NJS)
      PP=GAM*(H(NJS)-EL(NJS))/144.
      PPP=GAM*(H(N)-EL(N))/144.
      T=0.
      TT=0.
      K=0
      QINJ=0.
      WRITE(6,40) A,XL,D,VISC,PU,PD,PI,Q0,CDAU,CDAD,CDAI,G,TMAX,DT,B,N,
     1NJS,IPR,NDATA,RHO,PER,(TD(I),TAD(I),I=1,NDATA)
   40 FORMAT(' A,XL,D,VISC=',2F8.1,2E9.2/' PU,PD,PI,Q0=',3F8.2,E12.4/
     1' CDAU,CDAD,CDAI=',3E9.2/' G, TMAX, DT, B=',F8.3,2F8.4,F9.1/
     2' N, NJS, IPR, NDATA=',4I4/' RHO,PER,TD,TAD=',2F8.4/(2F8.5))
      WRITE(6,50)
   50 FORMAT('          P AND DISCHARGES ALONG THE PIPE'//
     1'    TIME X/L=      0.       INJ       1.       QINJ')
C BEGINNING OF TRANSIENT LOOP
   60 P1=(H(1)-EL(1))*GAM/144.
      P2=(H(NJS)-EL(NJS))*GAM/144.
      P3=(H(N)-EL(N))*GAM/144.
      Q1=Q(1)/Q0
      Q2=Q(NJS)/Q0
      Q3=Q(N)/Q0
      Q4=QINJ/Q0
      WRITE(6,70) T,P1,P2,P3,Q1,Q2,Q3,Q4
```

```
   70 FORMAT (1H ,F8.5,4H  P=,3F9.3,/10X,3H Q=,4F9.3)
   80 L=K/2+1
      TIME(L)=T
      PINJ(L)=GAM/144.*(H(NJS)-EL(NJS))-PP+24.
      PDS(L)=GAM/144.*(H(N)-EL(N))-PPP
      IF (T.GT.TMAX) GO TO 10
      II=2
   90 K=K+1
      T=T+DT
C COMPUTATION OF INTERIOR POINTS
      DO 110 I=II,N,2
      IF(I.EQ.NJS) GO TO 110
      CP=H(I-1)+Q(I-1)*B-HF(Q(I-1),D,AR,VISC,EPS,DX,G)
      QX=Q(I+1)
      HX=HF(Q(I+1),D,AR,VISC,EPS,DX,G)
      IF(I+1.NE.NJS)GO TO 100
      QX=Q(NS2)
      HX=HF(Q(NS2),D,AR,VISC,EPS,DX,G)
  100 CM=H(I+1)-QX*B+HX
      H(I)=.5*(CP+CM)
      Q(I)=(H(I)-CM)/B
  110 CONTINUE
      IF (II.EQ.3) GO TO 120
      II=3
      GO TO 90
C UPSTREAM BOUNDARY
  120 CM=H(2)-Q(2)*B+HF(Q(2),D,AR,VISC,EPS,DX,G)
      S=1.
      IF(HU-CM.LT.0.)S=-1.
      Q(1)=S*(-CV*B+SQRT(CV*B*CV*B+S*2.*CV*(HU-CM)))
      H(1)=CM+B*Q(1)
C DOWNSTREAM BOUNDARY
      CP=H(N)+Q(N)*B-HF(Q(N),D,AR,VISC,EPS,DX,G)
      S=1.
      IF(CP-HD.LT.0.)S=-1.
      Q(NS)=S*(-CVD*B+SQRT(CVD*CVD*B*B+S*2.*CVD*(CP-HD)))
      H(NS)=CP-B*Q(NS)
C INJECTOR BOUNDARY
C FIND INJECTOR FLOW
      TT=TT+DT*2./PER
      IF(TT.GT.1.) TT=TT-1.
      DO 130 I=2,NDATA
      KK=I-1
      IF(TD(I).GT.TT) GO TO 140
  130 CONTINUE
  140 TA=TAD(KK)+(TT-TD(KK))*(TAD(KK+1)-TAD(KK))/
     1(TD(KK+1)-TD(KK))
      CP=H(NJS-1)+Q(NJS-1)*B-HF(Q(NJS-1),D,AR,VISC,EPS,DX,G)
      CM=H(NJS+1)-Q(NJS+1)*B+HF(Q(NJS+1),D,AR,VISC,EPS,DX,G)
      A1=CP+CM+(B*CI*TA*.5)**2
      H(NJS)=.5*(A1-SQRT(A1*A1-(CP+CM)**2-(B*CI*TA)**2*HI))
      Q(NJS)=(-CM+H(NJS))/B
      Q(NS2)=(CP-H(NJS))/B
      QIO=QINJ
      QINJ=Q(NS2)-Q(NJS)
      VOL=VOL+DT*(QIO+QINJ)
      IF(TA.EQ.1.) QMAX=QINJ
      IF(K/IPR*IPR-K)80,60,80
  150 QAVE=VOL/PER
      WRITE(6,160) VOL,QAVE,QMAX
```

```
  160 FORMAT(' VOLUME INJECTED PER CYCLE=',F12.9/
     1' AVERAGE FLOW RATE OVER CYCLE=',F12.8/
     2' MAXIMUM FLOW RATE AT INJECTOR=',F12.8)
      IF(IPLT.EQ.1)CALL PLOT(TIME,PINJ,PDS,L,0.,-16.,.002,8.,10.,7.)
      STOP
      END
      FUNCTION HF(Q,D,AR,VISC,EPS,DX,G)
C  SUBROUTINE HF EVALUATES FRICTION FACTOR AND HEAD LOSS WITH COLEBROO
C FORMULA
      C1=EPS/D
      R=Q/AR*D/VISC
      IF(R.GT.2000.)GO TO 10
      FF=64./R
      GO TO 30
   10 FF=.02
C FIND FRICTION FACTOR
      DO 20 K=1,10
      F1=SQRT(FF)
      F=1./F1+0.86*ALOG(C1/3.7+2.51/R/F1)
      IF(ABS(F/FF).LE.0.01)GO TO 30
      DF=-0.5/F1**3*(1.+(2.51*.86/R/(C1/3.7+2.51/R/F1)))
      FF=FF-F/DF
   20 CONTINUE
   30   HF=FF*Q*ABS(Q)*DX/2./G/AR/AR/D
      RETURN
      END
 &DIN XL=29.2,A=4000.,D=.025417,G=32.2,EL=2*0.,60*3.28,
 PI=0.,CDAI=2.6E-6,
 PU=58368.,PD=32976.,RHO=1.5,CDAU=1.71E-5,CDAD=1.59E-5,VISC=.7E-5,
 TMAX=.005,N=56,NJS=19,IPR=2,NDATA=5,EPS=5.E-6,IPLT=0,
 PER=.05,TAD=0.,1.,1.,0.,0.,TD=0.,.01,.05,.055,1., &END
 /COMPILE
```

```
A,XL,D,VISC=  4000.0    29.2 0.25E-01 0.70E-05
PU,PD,PI,Q0=58368.0032976.00    0.00  0.2118E-02
CDAU,CDAD,CDAI= 0.17E-04 0.16E-04 0.26E-05
G, TMAX, DT, B=  32.200  0.0050  0.0001 244830.1
N, NJS, IPR, NDATA=  56  19   2   5
RHO,PER,TD,TAD=  1.5000  0.0500
0.00000 0.00000
0.01000 1.00000
0.05000 1.00000
0.05500 0.00000
1.00000 0.00000
      P AND DISCHARGES ALONG THE PIPE
   TIME X/L=      0.       INJ       1.       QINJ
 0.00000  P=   325.462  323.404  321.435
          Q=     1.000    1.000    1.000     0.000
 0.00026  P=   325.462  309.827  321.435
          Q=     1.000    0.922    1.000     0.156
 0.00052  P=   325.462  297.867  321.435
          Q=     1.000    0.853    1.000     0.294
 0.00078  P=   325.462  297.853  321.435
          Q=     1.000    0.853    1.000     0.294
 0.00104  P=   325.462  297.840  321.434
          Q=     1.000    0.853    1.000     0.294
 0.00130  P=   325.462  297.827  321.434
          Q=     1.000    0.853    1.000     0.294
 0.00156  P=   325.462  297.814  321.434
          Q=     1.000    0.853    1.000     0.294
 0.00182  P=   325.462  297.800  321.434
          Q=     1.000    0.853    1.000     0.294
 0.00209  P=   325.462  297.787  321.434
          Q=     1.000    0.853    1.000     0.294
 0.00235  P=   325.462  297.774  321.434
          Q=     1.000    0.853    1.000     0.294
 0.00261  P=   312.264  308.441  321.433
          Q=     1.079    0.915    1.000     0.171
 0.00287  P=   300.237  323.278  321.433
          Q=     1.147    1.000    1.000     0.000
 0.00313  P=   300.230  323.278  321.433
          Q=     1.147    1.000    1.000     0.000
 0.00339  P=   300.224  323.278  321.433
          Q=     1.147    1.000    1.000     0.000
 0.00365  P=   300.219  323.278  321.433
          Q=     1.147    1.000    1.000     0.000
 0.00391  P=   300.212  323.278  321.433
          Q=     1.147    1.000    1.000     0.000
 0.00417  P=   300.206  323.278  321.432
          Q=     1.147    1.000    1.000     0.000
 0.00443  P=   300.200  323.278  321.432
          Q=     1.147    1.000    1.000     0.000
 0.00469  P=   300.194  323.278  321.432
          Q=     1.147    1.000    1.000     0.000
 0.00495  P=   310.950  323.587  321.432
          Q=     1.087    1.002    1.000     0.000
 0.00521  P=   325.407  323.458  307.986
          Q=     1.000    1.001    0.923     0.000
VOLUME INJECTED PER CYCLE= 0.000001477
AVERAGE FLOW RATE OVER CYCLE=  0.00002954
MAXIMUM FLOW RATE AT INJECTOR=  0.00062167
```

LIST OF VARIABLES

MAIN PROGRAM, LAMINAR FLOW

A: pressure wave propagation velocity

AR: pipe cross-sectional area

AI: miscellaneous collection of variables

B: pipeline characteristic impedance, B=A/(G*AR)

CDAD: product of downstream orifice discharge coefficient and flow area

CDAI: product of injector discharge coefficient and flow area

CDAU: producte of upstream orifice discharge coefficient and flow area

CI: = $CDAI\sqrt{2g}$

CM,CP: collection of variables in C^+ and C^- compatibility equations

CV: = $g(CDAU)^2$

CVD: = $g(CDAD)^2$

D: pipe diameter

DIN: namelist name

DT: time-step size = $\Delta x/A$

EL: elevation of sections above reference datum

FC: coefficient in the unsteady friction term

G: acceleration of gravity

GAM: unit weight of fluid = ρg

H: hydraulic grade line elevation above reference datum, $H = EL + p/\rho g$

HB: = RQ_N, normal viscous friction loss at section N

HD: constant pressure head outside the downstream orifice

HF: total friction loss at a section

HFF: vector to store components of friction term (for printout only)

HI: constant hydraulic gradeline elevation outside the injector

HP: unsteady portion of the total friction loss at section N

HU: constant pressure head on the upstream side of the upstream orifice

HX: temporary storage of HF(NS2) for calculation of CM at the section upstream from injector

I: integer usually used to identify pipe section

IDIAG: = 1 to printout frequency dependent friction diagnostic information

= 0 for no printout

II: refers to the first upstream section at which interior point calculations are carried out: = 2 when K is odd, = 3 when K is even

III: = II - 1

IPLT: = 1 to obtain a plot of pressures

= 0 for no plot

IPR: controls number of pairs of time steps to be computed between print out; must be even

K: integer counter identifying the number of time steps

KF,KK: integers

KMAX: number of terms used in unsteady friction

KMI: = KMAX + 1

L: integer that counts the number of points to be plotted

N: number of reaches in system between upstream and downstream orifices

NDATA: number of pairs of values of τ and t to describe the injector pulse

NJS: section number of injector location

NS: = N + 1

N2Z: = NS + 1; subscript location to store information at upstream side of injector in main pipe

PD: pressure at downstream side of downstream orifice

PDS: vector to store downstream pressure to plot

PER: period of injector pulse

PI: pressure outside the injector

PINJ: vector to store pressure in fuel rail at the injector

PP,PPP: initial pressure at downstream orifice and injector respectively

PU: constant pressure upstream from upstream orifice

P1,P2,P3: used for print out of pressures

Q: volumetric flow rate at sections

QAVE: volumetric flow rate at injector averaged over entire period

QF: volumetric flow rate stored as a function of time at each section

QINJ: injector volumetric flow rate, current

QIO: injector volumetric flow rate, 2 time steps earlier

QMAX: maximum instantaneous flow rate at injector

QX: temporary storage of Q for calculations of CM

QO: initial steady-state volumetric flow rate

Q1,Q2,Q3,Q4: dimensionless flow rates for print out

R: steady-state resistance factor

RHO: mass density of fluid

S: $= \pm 1$ to designate sign of flow direction

T: time

TA: dimensionless number, τ, to describe the injector needle position

TAD: tabular input values of τ vs time, TD, to describe injector motion during cycle

TD: dimensionless time, t/PER, tabular values paired with TAD

TIME: vector to store time corresponding to PINJ and PDS to plot

TMAX: duration of transient simulation in seconds

TT: dimensionless time during each injector cycle

VISC: kinematic viscosity

VOL: volume of fluid injected during each cycle

W: weighting function used in unsteady friction evaluation

XL: length of pipe between orifices

Subroutine Weight

K: integer counter

ST: $\sqrt{TAU}$

TAU: dimensionless time used in weighting function

$= 4\nu t/D^2$

TAU1: $= 4\nu/D^2$

Main Program; Turbulent Flow

Additional variables not used in laminar flow program

DX: = XL/N, length of each reach

EPS: linear dimension of surface roughness of pipe

Function HF, used in Turbulent Flow Program

C1: = EPS/D, dimensionless roughness

DF: derivative of Colebrook equation

F: designation of Colebrook equation

FF: Darcy Weisbach friction factor

FI: = $\sqrt{FF}$

R: Reynolds number = VD/V

AIIM SCANNER TEST CHART # 2

Spectra

4 PT ABCDEFGHIJKLMNOPQRSTUVWXYZabcdefghijklmnopqrstuvwxyz;:",./?$0123456789
6 PT ABCDEFGHIJKLMNOPQRSTUVWXYZabcdefghijklmnopqrstuvwxyz;:",./?$0123456789
8 PT ABCDEFGHIJKLMNOPQRSTUVWXYZabcdefghijklmnopqrstuvwxyz;:",./?$0123456789
10 PT ABCDEFGHIJKLMNOPQRSTUVWXYZabcdefghijklmnopqrstuvwxyz;:",./?$0123456789

Times Roman

4 PT ABCDEFGHIJKLMNOPQRSTUVWXYZabcdefghijklmnopqrstuvwxyz;:",./?$0123456789
6 PT ABCDEFGHIJKLMNOPQRSTUVWXYZabcdefghijklmnopqrstuvwxyz;:",./?$0123456789
8 PT ABCDEFGHIJKLMNOPQRSTUVWXYZabcdefghijklmnopqrstuvwxyz;:",./?$0123456789
10 PT ABCDEFGHIJKLMNOPQRSTUVWXYZabcdefghijklmnopqrstuvwxyz;:",./?$0123456789

Century Schoolbook Bold

4 PT ABCDEFGHIJKLMNOPQRSTUVWXYZabcdefghijklmnopqrstuvwxyz;:",./?$0123456789
6 PT ABCDEFGHIJKLMNOPQRSTUVWXYZabcdefghijklmnopqrstuvwxyz;:",./?$0123456789
8 PT ABCDEFGHIJKLMNOPQRSTUVWXYZabcdefghijklmnopqrstuvwxyz;:",./?$0123456789
10 PT ABCDEFGHIJKLMNOPQRSTUVWXYZabcdefghijklmnopqrstuvwxyz;:",./?$0123456789

News Gothic Bold Reversed

4 PT ABCDEFGHIJKLMNOPQRSTUVWXYZabcdefghijklmnopqrstuvwxyz;:",./?$0123456789
6 PT ABCDEFGHIJKLMNOPQRSTUVWXYZabcdefghijklmnopqrstuvwxyz;:",./?$0123456789
8 PT ABCDEFGHIJKLMNOPQRSTUVWXYZabcdefghijklmnopqrstuvwxyz;:",./?$0123456789
10 PT ABCDEFGHIJKLMNOPQRSTUVWXYZabcdefghijklmnopqrstuvwxyz;:",./?$0123456789

Bodoni Italic

4 PT ABCDEFGHIJKLMNOPQRSTUVWXYZabcdefghijklmnopqrstuvwxyz;:",./?$0123456789
6 PT ABCDEFGHIJKLMNOPQRSTUVWXYZabcdefghijklmnopqrstuvwxyz;:",./?$0123456789
8 PT ABCDEFGHIJKLMNOPQRSTUVWXYZabcdefghijklmnopqrstuvwxyz;:",./?$0123456789
10 PT ABCDEFGHIJKLMNOPQRSTUVWXYZabcdefghijklmnopqrstuvwxyz;:",./?$0123456789

Greek and Math Symbols

4 PT ΑΒΓΔΕΞΘΗΙΚΛΜΝΟΠΦΡΣΤΥΩΧΨΖαβγδεξθηικλμνοπφρστυωχψζ≧∓",./≦±=≠°><⊁⊀⋗⋖≡
6 PT ΑΒΓΔΕΞΘΗΙΚΛΜΝΟΠΦΡΣΤΥΩΧΨΖαβγδεξθηικλμνοπφρστυωχψζ≧∓",./≦±=≠°><⊁⊀⋗⋖≡
8 PT ΑΒΓΔΕΞΘΗΙΚΛΜΝΟΠΦΡΣΤΥΩΧΨΖαβγδεξθηικλμνοπφρστυωχψζ≧∓",./≦±=≠°><⊁⊀⋗⋖≡
10 PT ΑΒΓΔΕΞΘΗΙΚΛΜΝΟΠΦΡΣΤΥΩΧΨΖαβγδεξθηικλμνοπφρστυωχψζ≧∓",./≦±=≠°><⊁⊀⋗⋖≡

White

Black

Isolated Characters

e	m	1	2	3	a
4	5	6	7	o	°
8	9	0	h	I	B

0123456 6543210 A4 Page 6543210

MESH HALFTONE WEDGES

65

85

100

110

133

150

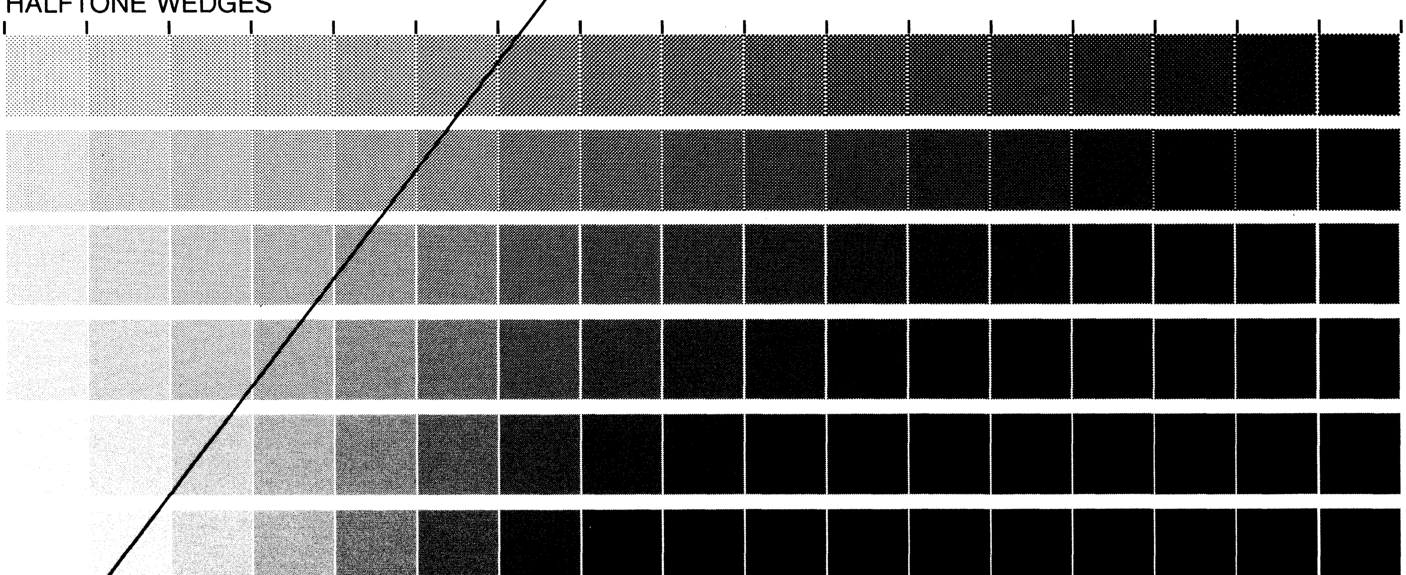

RIT ALPHANUMERIC RESOLUTION TEST OBJECT, RT-1-71

PRODUCED BY GRAPHIC ARTS RESEARCH CENTER

ROCHESTER INSTITUTE OF TECHNOLOGY, ONE LOMB

MEMORIAL DRIVE, ROCHESTER, NEW YORK 14623